

## Electronic Supporting Information

### SNS Ligand-Assisted Catalyst Activation in Zn-Catalysed Carbonyl Hydroboration

Saeed Ataie,<sup>[a]</sup> Seth Hogeterp,<sup>[a]</sup> Jeffrey S. Ovens,<sup>[b]</sup> and R. Tom Baker\*<sup>[a]</sup>

---

[a] S. Ataie, S. Hogeterp, R. T. Baker  
Department of Chemistry and Biomolecular Sciences and Centre for Catalysis Research and Innovation  
University of Ottawa  
Ottawa, Ontario K1N 6N5 Canada  
E-mail: rbaker@uottawa.ca

[b] Dr. J. A. Ovens  
Faculty of Science  
University of Ottawa  
Ottawa, Ontario K1N 6N5 Canada

#### Table of Contents

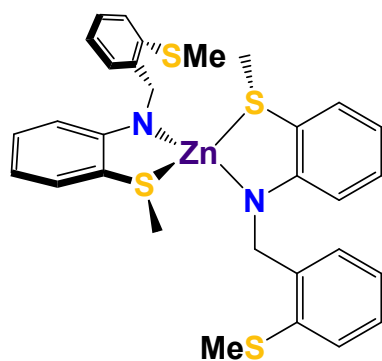
1. General Details	S2
2. Synthesis and Characterization	S2
3. Catalysis Protocols	S4
4. Mechanistic Studies	S5
5. NMR and EI-MS Spectra	S8
6. Monitoring Acetophenone Hydroboration Reactions Using Zinc Complexes	S22
7. EI-MS Spectra of Complexes	S23
8. X-ray Diffraction Data	S25
9. References	S32

## 1. General Details

All experiments were carried out under a dry nitrogen atmosphere using Schlenk techniques or an MBraun glovebox unless otherwise stated. Hexane, diethyl ether, and THF were dried on columns of activated alumina using a J. C. Meyer solvent purification system. Benzene- $d_6$  ( $C_6D_6$ ) was dried by standing over activated alumina (ca. 10 wt %). All solvents were stored over activated (heated at ca. 250 °C for >10 h under vacuum) 4 Å molecular sieves, except ethanol which was stored over activated 3 Å molecular sieves. Glassware was oven-dried at 160 °C for >1 h. The following chemicals were obtained commercially, as indicated: zinc chloride (Alfa Aesar, 99.98%), dichloromethane (HPLC grade,  $\geq 99.8\%$ , contains amylene as stabilizer), ethanol (anhydrous,  $\leq 0.005\%$  water) and  $Li[N(SiMe_3)_2]$  (Sigma Aldrich, 97%).  $^1H$ ,  $^{13}C$ ,  $^{11}B$ , and HSQC NMR spectra were recorded on a 300 MHz Bruker Avance II instrument at room temperature.  $^1H$  and  $^{13}C\{^1H\}$  NMR spectra were referenced to residual protons and solvent carbons ( $C_6D_6$ ,  $\delta$  7.13, 127.66 ppm;  $CDCl_3$ ,  $\delta$  7.26, 77.02 ppm). Proligands  $HL^1$  and  $HL^2$  and Zn bis(alkoxide) complex **1** were prepared according to literature procedures.<sup>[1-3]</sup> For electron impact (EI), solid samples were prepared by drying products under vacuum, and spectra obtained using a Kratos Concept S1 instrument (Hres 7000–10000). X-ray diffraction data were collected on a Bruker Smart or Kappa diffractometer equipped with an ApexII CCD detector and a sealed-tube Mo K source ( $\lambda = 0.71073$  Å).

## 2. Synthesis and Characterization

### 2.1 Preparation of $[Zn(\kappa^2-S^{Me}N-S^{Me})_2]$ , ( $Zn(L^1)_2$ )

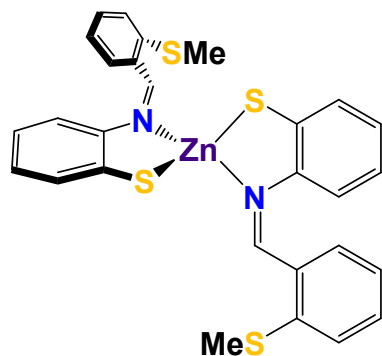


A 42 mL vial was charged with 2-(2-methylthiobenzyl)-methylthioaniline,  $[S^{Me}NHS^{Me}]$  (0.201 g, 0.73 mmol),  $Li[N(SiMe_3)_2]$  (0.122 g, 0.73 mmol) and 15 mL of THF, and then a solution of  $ZnCl_2$  (0.05 g, 0.37 mmol, in 5 mL of THF) was added gradually, yielding a yellowish solution that was stirred overnight at room temperature. Afterward, the solvent was pumped off under vacuum and the residue extracted into benzene and filtered. After removing the benzene under vacuum the resulting precipitate was washed

with diethyl ether multiple times and then crystallized from DCM at -35 °C. The crystalline product was then filtered and dried in vacuo. Yield: 0.156 g, 69% based on  $ZnCl_2$ . Crystals of  $Zn(L^1)_2$  suitable for X-ray crystallography were obtained by layering a DCM solution of  $Zn(L^1)_2$  with hexane.

**$^1H$  NMR (300 MHz,  $CDCl_3$  at 25 °C):**  $\delta$  2.18 (s, 6H, S-Me), 2.43 (s, 6H, S-Me), 4.19 (s, 4H, N- $CH_2$ ), 6.34 (m, 4H, Ar-H), 6.91 (td, 2H, Ar-H), 7.12 (m, 8H, Ar-H), 7.3 (dd, 2H, Ar-H).  **$^{13}C\{^1H\}$  NMR (75 MHz,  $CDCl_3$ , 25 °C):** 15.1 (s, 2C, S- $CH_3$ ); 21.9 (s, 2C, S- $CH_3$ ); 51.4 (s, 2C, N- $CH_2$ ); 111.0 (s, 2C, ArSNS-C); 111.7 (s, 2C, ArSNS-C); 113.6 (s, 2C, ArSNS-C); 124.3 (s, 2C, ArSNS-C); 124.5 (s, 2C, ArSNS-C); 127.4 (s, 2C, ArSNS-C); 128.0 (s, 2C, ArSNS-C); 131.9 (s, 2C, ArSNS-C); 135.0 (s, 2C, ArSNS-C); 137.4 (s, 2C, ArSNS-C); 138.7 (s, 2C, ArSNS-C); 156.5 ppm (s, 2C, ArSNS-C) (Figures S1 and S2).

## 2.2 Preparation of $[\text{Zn}(\kappa^2\text{-SNS}^{\text{Me}})_2]$ , $(\text{Zn}(\text{L}^2)_2)$



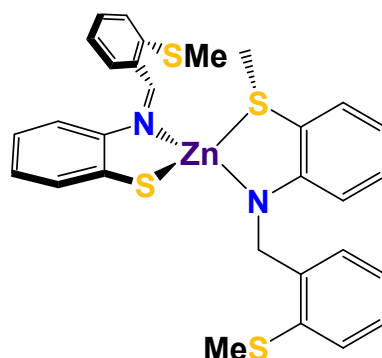
A 42 mL vial was charged with 2-(2-methylthiophenyl)-benzothiazolidine (0.190 g, 0.73 mmol),  $\text{Li}[\text{N}(\text{SiMe}_3)_2]$  (0.122 g, 0.73 mmol) and 15 mL of THF, and then a solution of  $\text{ZnCl}_2$  (0.05 g, 0.37 mmol, in 5 mL of THF) was added gradually, giving a red solution. The resulting solution was stirred overnight at room temperature, yielding a red precipitate that was filtered, washed with THF (2 times) and diethyl ether (multiple times) and then recrystallized from hot THF. Finally, the recrystallized product was filtered and dried under vacuum. Yield: 0.158 g, 74% based on

$[\text{ZnCl}_2]$ . Crystals of  $\text{Zn}(\text{L}^2)_2$  suitable for X-ray crystallography were obtained by layering a DCM solution of  $\text{Zn}(\text{L}^2)_2$  with hexane.

**$^1\text{H}$  NMR (300 MHz,  $\text{CDCl}_3$  at 25 °C):**  $\delta$  2.47 (s, 6H, S-Me), 6.49 (td, 2H, Ar-H), 7.02 (m, 6H, Ar-H), 7.28 (m, 4H, Ar-H), 7.44 (dd, 2H, Ar-H), 7.61 (dd, 2H, Ar-H), 9.06 (s, 2H, N=CH).

**$^{13}\text{C}\{^1\text{H}\}$  NMR (75 MHz,  $\text{CDCl}_3$ , 25 °C):** 17.1 (s, 2C, S-CH<sub>3</sub>); 119.2 (s, 2C, ArSNS-C); 122.7 (s, 2C, ArSNS-C); 125.4 (s, 2C, ArSNS-C); 127.5 (s, 2C, ArSNS-C); 128.7 (s, 2C, ArSNS-C); 129.5 (s, 2C, ArSNS-C); 132.9 (s, 2C, ArSNS-C); 133.0 (s, 2C, ArSNS-C); 133.7 (s, 2C, ArSNS-C); 141.4 (s, 2C, ArSNS-C); 144.4 (s, 2C, ArSNS-C); 146.4 (s, 2C, ArSNS-C); 163.1 ppm (s, 2C, N=C) (Figures S3 and S4).

## 2.3 Preparation of $[\text{Zn}(\kappa^2\text{-S}^{\text{Me}}\text{N-S}^{\text{Me}})(\kappa^2\text{-S-NS}^{\text{Me}})]$ , $\text{Zn}(\text{L}^1)(\text{L}^2)$



A 42 mL vial was charged with  $\text{ZnCl}_2$  (0.138 g, 1.02 mmol) in 5 mL of THF and then a solution of 2-(2-methylthiobenzyl)-methylthioaniline (0.280 g, 1.02 mmol) and  $\text{Li}[\text{N}(\text{SiMe}_3)_2]$  (0.170 g, 1.02 mmol) in 15 mL of THF was added gradually, giving a yellowish solution. The resulting solution was stirred for 3 h at room temperature. Then a solution of 2-(2-methylthiophenyl)-benzothiazolidine (0.263 g, 1.02 mmol) and  $\text{Li}[\text{N}(\text{SiMe}_3)_2]$  (0.170 g, 1.02 mmol) in 15 mL of THF was added, yielding an orange solution with precipitate after 1 h. The mixture was stirred for 2 h

and filtered, washed with diethyl ether and dried under vacuum. Yield: 0.458 g, 75% based on  $\text{ZnCl}_2$ . Crystals of  $\text{Zn}(\text{L}^1)(\text{L}^2)$  suitable for X-ray crystallography were obtained by layering a DCM solution of  $\text{Zn}(\text{L}^1)(\text{L}^2)$  with hexane.

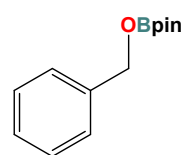
**$^1\text{H}$  NMR (300 MHz,  $\text{CDCl}_3$ , 25 °C):**  $\delta$  2.27 (s, 3H, S-Me), 2.35 (s, 3H, S-Me), 2.52 (s, 3H, S-Me) 4.06 (dd, 2H, N-CH<sub>2</sub>), 6.29 (td, 1H, Ar-H), 6.43 (dd, 1H, Ar-H), 6.84 (td, 1H, Ar-H), 7.02 (m, 7H, Ar-H), 7.16 (dt, 2H, Ar-H), 7.29 (m, 2H, Ar-H), 7.45 (d, 2H, Ar-H).  **$^{13}\text{C}\{^1\text{H}\}$  NMR (75 MHz,  $\text{CDCl}_3$ , 25 °C):** 15.6 (s, 1C, S-CH<sub>3</sub>); 16.9 (s, 1C, S-CH<sub>3</sub>); 22.3 (s, 1C, S-CH<sub>3</sub>); 51.5 (s, 1C, N-CH<sub>2</sub>); 111.4 (s, 1C, ArSNS-C); 111.5 (s, 1C, ArSNS-C); 114.2 (s, 1C, ArSNS-C); 119.0 (s, 1C, ArSNS-C); 122.7 (s, 1C, ArSNS-C); 124.8 (s, 1C, ArSNS-C); 125.4 (s, 1C, ArSNS-C); 125.5 (s, 1C, ArSNS-C); 126.8 (s, 1C, ArSNS-C); 127.8 (s, 1C, ArSNS-C); 128.6 (s, 1C, ArSNS-C); 129.0 (s, 1C, ArSNS-C); 129.5 (s, 1C, ArSNS-C); 132.0 (s, 1C, ArSNS-C); 132.3 (s, 1C,

ArSNS-C); 132.8 (s, 1C, ArSNS-C); 133.3 (s, 1C, ArSNS-C); 135.4 (s, 1C, ArSNS-C); 138.2 (s, 1C, ArSNS-C); 138.7 (s, 1C, ArSNS-C); 141.4 (s, 1C, ArSNS-C); 143.4 (s, 1C, ArSNS-C); 146.5 (s, 1C, ArSNS-C); 156.1 (s, 1C, ArSNS-C); 161.8 ppm (s, 1C, N=C) (Figures S5 and S6).

### 3. Catalysis protocols

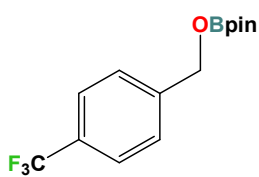
A stock solution of  $\text{Zn}(\text{L}^1)(\text{L}^2)$  was prepared by dissolving 6 mg  $\text{Zn}(\text{L}^1)(\text{L}^2)$  in 5 mL of  $\text{C}_6\text{D}_6$ . A vial containing the appropriate amount of catalyst [ $\text{Zn}(\text{L}^1)_2$  (6 mg, 1 mol%),  $\text{Zn}(\text{L}^2)_2$  (6 mg, 1 mol%),  $\text{Zn}(\text{L}^1)(\text{L}^2)$  (6 mg, 1 mol%), or 0.5 mL of stock solution of  $\text{Zn}(\text{L}^1)(\text{L}^2)$  (0.6 mg, 0.1 mol%)], was charged with 0.5 mL  $\text{C}_6\text{D}_6$ , 1.0 mmol of carbonyl substrate (102  $\mu\text{L}$  of benzaldehyde or 116  $\mu\text{L}$  of acetophenone), and subsequently with 1.0 mmol of pinacolborane (145  $\mu\text{L}$ ), resulting in a color change from red  $\text{Zn}(\text{L}^2)_2$ , pale-yellow  $\text{Zn}(\text{L}^1)_2$  or orange  $\text{Zn}(\text{L}^1)(\text{L}^2)$  to colorless. The rate of color change for  $\text{Zn}(\text{L}^1)(\text{L}^2)$  was extremely fast, for  $\text{Zn}(\text{L}^1)_2$  was relatively fast, and for  $\text{Zn}(\text{L}^2)_2$  was slow. The solution was charged to an NMR tube for further analysis. Reaction times varied slightly from 5-30 minutes. Yield was determined by  $^1\text{H}$  NMR in reference to internal standard mesitylene.

#### 3.1 Hydroboration of benzaldehyde



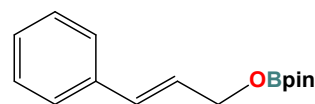
Following the general procedure, benzaldehyde (102  $\mu\text{L}$ , 1.0 mmol), pinacolborane (145  $\mu\text{L}$ , 1.0 mmol), and either  $\text{Zn}(\text{L}^1)_2$  (6 mg, 1 mol%), or  $\text{Zn}(\text{L}^2)_2$  (6 mg, 1 mol%), or  $\text{Zn}(\text{L}^1)(\text{L}^2)$  (6 mg, 1 mol%) were used.  $^1\text{H}$  NMR showed quantitative conversion to hydroboration product after 5 min for  $\text{Zn}(\text{L}^1)_2$  and  $\text{Zn}(\text{L}^2)_2$ , and 15 sec for  $\text{Zn}(\text{L}^1)(\text{L}^2)$  at room temperature.  $^{11}\text{B}$  and  $^1\text{H}$  NMR shifts matched with literature values (Figure S17).<sup>[4]</sup>

#### 3.2 Hydroboration of 4-trifluoromethylbenzaldehyde



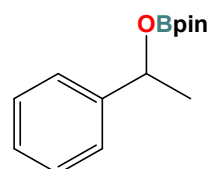
Following the general procedure, 4-trifluoromethylbenzaldehyde (137  $\mu\text{L}$ , 1.0 mmol), pinacolborane (145  $\mu\text{L}$ , 1.0 mmol), and either  $\text{Zn}(\text{L}^1)_2$  (6 mg, 1 mol%), or  $\text{Zn}(\text{L}^2)_2$  (6 mg, 1 mol%) were used.  $^1\text{H}$  NMR showed quantitative conversion to hydroboration product after 5 min, at room temperature (Figure S18).

#### 3.3 Hydroboration of cinnamaldehyde



Following the general procedure, cinnamaldehyde (126  $\mu\text{L}$ , 1.0 mmol), pinacolborane (145  $\mu\text{L}$ , 1.0 mmol), and either  $\text{Zn}(\text{L}^1)_2$  (6 mg, 1 mol%), or  $\text{Zn}(\text{L}^2)_2$  (6 mg, 1 mol%) were used.  $^1\text{H}$  NMR showed quantitative conversion to hydroboration product after 5 min at room temperature (Figure S19).

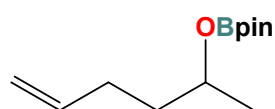
#### 3.4 Hydroboration of acetophenone



Following the general procedure, acetophenone (116  $\mu\text{L}$ , 1.0 mmol), pinacolborane (145  $\mu\text{L}$ , 1.0 mmol), and either  $\text{Zn}(\text{L}^1)_2$  (6 mg, 1 mol%), or  $\text{Zn}(\text{L}^2)_2$

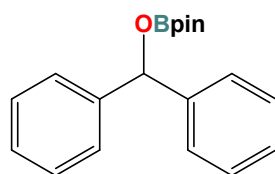
(6 mg, 1 mol%), or  $\text{Zn}(\text{L}^1)(\text{L}^2)$  (6 mg, 1 mol%), or 0.5 mL of stock solution of  $\text{Zn}(\text{L}^1)(\text{L}^2)$  (0.6 mg, 0.1 mol%) were used.  $^1\text{H}$  NMR showed quantitative conversion to hydroboration product after 25 min for  $\text{Zn}(\text{L}^1)_2$  and  $\text{Zn}(\text{L}^2)_2$ , 15 sec for  $\text{Zn}(\text{L}^1)(\text{L}^2)$  (1 mol%), and 16 min for  $\text{Zn}(\text{L}^1)(\text{L}^2)$  (0.1 mol%) at room temperature.  $^{11}\text{B}$  and  $^1\text{H}$  NMR shifts matched with literature values (Figure S20).<sup>[4]</sup>

### 3.5 Hydroboration of 5-hexen-2-one



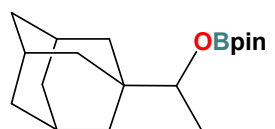
Following the general procedure, 5-hexen-2-one (116  $\mu\text{L}$ , 1.0 mmol), pinacolborane (145  $\mu\text{L}$ , 1.0 mmol), and either  $\text{Zn}(\text{L}^1)_2$  (6 mg, 1 mol%), or  $\text{Zn}(\text{L}^2)_2$  (6 mg, 1 mol%) were used.  $^1\text{H}$  NMR showed quantitative conversion to hydroboration product after 20 min, at room temperature (Figure S21).

### 3.6 Hydroboration of benzophenone



Following the general procedure, benzophenone (182 mg, 1.0 mmol), pinacolborane (145  $\mu\text{L}$ , 1.0 mmol), and either  $\text{Zn}(\text{L}^1)_2$  (6 mg, 1 mol%), or  $\text{Zn}(\text{L}^2)_2$  (6 mg, 1 mol%) were used.  $^1\text{H}$  NMR showed quantitative conversion to hydroboration product after 28 min, at room temperature (Figure S22).

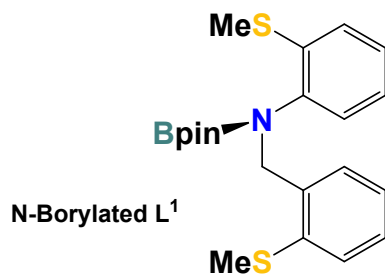
### 3.7 Hydroboration of 1-adamantyl methyl ketone



Following the general procedure, cinnamaldehyde (178 mg, 1.0 mmol), pinacolborane (145  $\mu\text{L}$ , 1.0 mmol), and either  $\text{Zn}(\text{L}^1)_2$  (6 mg, 1 mol%), or  $\text{Zn}(\text{L}^2)_2$  (6 mg, 1 mol%) were used.  $^1\text{H}$  NMR showed quantitative conversion to hydroboration product after 25 min, at room temperature (Figure S23).

## 4. Mechanistic Studies

### 4.1 Stoichiometric reaction of $\text{Zn}(\text{L}^1)_2$ with HBpin: Formation of *N*-borylated $\text{L}^1$



*N*-Borylated  $\text{L}^1$

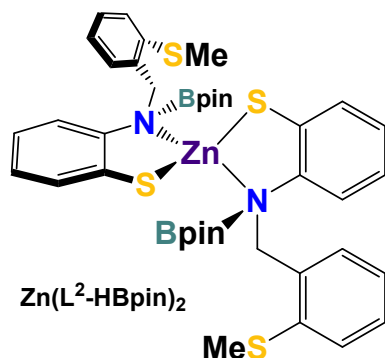
A pale-yellow solution of  $\text{Zn}(\text{L}^1)_2$  (0.05 g, 0.08 mmol) in  $\text{C}_6\text{D}_6$  was charged with pinacolborane (11.5  $\mu\text{L}$ , 0.08 mmol), resulting in a fast color change to almost colorless. The crude  $^1\text{H}$  NMR spectrum showed half of  $\text{Zn}(\text{L}^1)_2$  was converted into a new compound and half remained as  $\text{Zn}(\text{L}^1)_2$ , and also a light grey precipitate was formed. Increasing the amount of pinacolborane to 2 equiv (23  $\mu\text{L}$ , 0.16 mmol) gave full conversion of  $\text{Zn}(\text{L}^1)_2$ . The light grey precipitate was filtered off and the filtrate evaporated slowly. After

2 days colorless crystals were formed. The  $^1\text{H}$  and  $^{11}\text{B}$  NMR spectra and X-ray diffraction study revealed the product to be *N*-borylated  $\text{L}^1$  (Figures S7 and S8).

$^1\text{H}$  NMR (300 MHz,  $\text{C}_6\text{D}_6$  at 25  $^\circ\text{C}$ ):  $\delta$  1.17 (s, 12H, Bpin Me), 1.83 (s, 3H, S-Me), 1.97 (s, 3H, S-Me), 5.07 (s, 2H, N- $\text{CH}_2$ ), 6.68 (td, 1H, Ar-H), 6.80 (td, 1H, Ar-H), 6.88 (dd, 1H, Ar-H), 6.96

(m, 3H, Ar-H), 7.03 (dd, 1H, Ar-H), 7.62 (m, 1H, Ar-H).  $^{11}\text{B}\{^1\text{H}\}$  NMR (96 MHz,  $\text{C}_6\text{D}_6$ , 25 °C): 24.1 ppm (s).

#### 4.2 Stoichiometric reaction of $\text{Zn}(\text{L}^2)_2$ with HBpin: Formation of $\text{Zn}(\text{L}^2\text{-HBpin})_2$

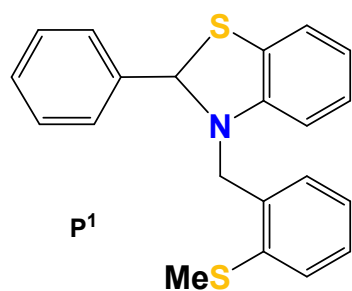


A red suspension of  $\text{Zn}(\text{L}^2)_2$  (0.05 g, 0.085 mmol) in  $\text{C}_6\text{D}_6$  was charged with pinacolborane (12.5  $\mu\text{L}$ , 0.085 mmol), giving a homogeneous light orange solution after 3 h. The crude  $^1\text{H}$  NMR spectrum showed half of  $\text{Zn}(\text{L}^2)_2$  was converted into a new species and half remained as  $\text{Zn}(\text{L}^2)_2$ . Increasing the amount of pinacolborane to 2 equiv (23  $\mu\text{L}$ , 0.16 mmol) resulted in a slow decolourisation and complete conversion of  $\text{Zn}(\text{L}^2)_2$  was confirmed by  $^1\text{H}$  NMR. The solvent was then removed under vacuum and the residue washed with hexane and filtered. The  $^1\text{H}$  NMR spectrum

of  $\text{Zn}(\text{L}^2\text{-HBpin})_2$  showed broad resonances that sharpened significantly at 45 °C (Figure S9). All attempts at growing a crystal of  $\text{Zn}(\text{L}^2\text{-HBpin})_2$  were unsuccessful.

$^1\text{H}$  NMR (300 MHz,  $\text{C}_6\text{D}_6$ , 45 °C):  $\delta$  1.24 (s, 24H, Bpin Me), 2.00 (s, 6H, S-Me), 4.91 (s, 4H, N- $\text{CH}_2$ ), 6.68 (m, 4H, Ar-H), 6.83 (m, 6H, Ar-H), 6.98 (m, 4H, Ar-H), 7.75 (s, 2H, Ar-H).  $^{13}\text{C}\{^1\text{H}\}$  NMR (75 MHz,  $\text{C}_6\text{D}_6$ , 45 °C): 15.9 (S-Me); 24.3 (Bpin Me); 50.3 (N- $\text{CH}_2$ ); 82.4 (Bpin); 110.9 (ArSNS-C); 118.5 (ArSNS-C); 124.5 (ArSNS-C); 125.5 (ArSNS-C); 127.0 (ArSNS-C); 129.9 (ArSNS-C); 130.9 (ArSNS-C); 134.6 (ArSNS-C); 136.1 (ArSNS-C); 137.1 (ArSNS-C); 144.5 ppm (ArSNS-C).  $^{11}\text{B}\{^1\text{H}\}$  NMR (96 MHz,  $\text{C}_6\text{D}_6$ , 45 °C): 21.1 ppm (Figures S10 and S11). EI-MS showed  $(\text{L}^2\text{-HBpin})^+$  Calc'd for  $[\text{C}_{21}\text{H}_{27}\text{BNO}_2\text{S}_2]$  387.15, Found 387.2 (Figure S12).

#### 4.3 Stoichiometric reaction of $\text{Zn}(\text{L}^2\text{-HBpin})_2$ with benzaldehyde: Formation of $\text{P}^1$

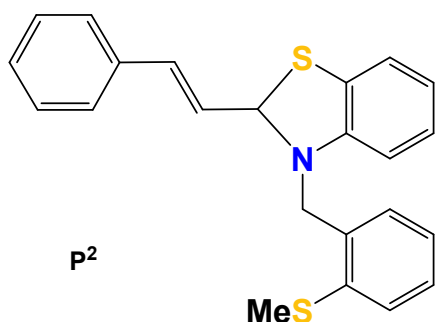


After the reaction in 4.2 (1 equiv of  $\text{Zn}(\text{L}^2)_2$  and 2 equiv of pinacolborane in  $\text{C}_6\text{D}_6$ ) became colorless and  $\text{Zn}(\text{L}^2\text{-HBpin})_2$  was formed, 2 equiv of benzaldehyde (17  $\mu\text{L}$ , 0.17 mmol) was added to the reaction mixture, resulting immediately in a pale yellow solution. After 3 h the solvent was evaporated under vacuum and the residue was washed with hexane and filtered.  $^1\text{H}$  NMR of both solid and filtrate showed no hydroborated product, but the latter showed a new

product ( $\text{P}^1$ ). This benzothiazoline product was isolated using column chromatography and characterized by  $^1\text{H}$  and  $^{13}\text{C}$  NMR, and X-ray crystallography (Figures S13 and S14)

$^1\text{H}$  NMR (300 MHz,  $\text{CDCl}_3$  at 25 °C):  $\delta$  2.45 (s, 3H, S-Me), 4.31 (q, 2H, N- $\text{CH}_2$ ), 6.24 (s, 1H, N-CHR-S), 6.29 (dd, 1H, Ar-H), 6.73 (td, 1H, Ar-H), 6.96 (td, 1H, Ar-H), 7.11 (m, 2H, Ar-H); 7.30 (m, 6H, Ar-H), 7.48 (m, 2H, Ar-H).  $^{13}\text{C}\{^1\text{H}\}$  NMR (75 MHz,  $\text{CDCl}_3$ , 25 °C): 15.8 (S-Me); 48.5 (N- $\text{CH}_2$ ); 74.3 (N-C-S); 107.7 (ArSNS-C); 119.1 (ArSNS-C); 121.4 (ArSNS-C); 125.0 (ArSNS-C); 125.5 (ArSNS-C); 125.7 (ArSNS-C); 125.7 (ArSNS-C); 127.2 (ArSNS-C); 127.3 (ArSNS-C); 127.7 (ArSNS-C); 128.7 (ArSNS-C); 128.9 (ArSNS-C); 134.3 (ArSNS-C); 136.9 (ArSNS-C); 140.3 (ArSNS-C); 147.0 ppm (ArSNS-C).

#### 4.4 Stoichiometric reaction of $\text{Zn}(\text{L}^2\text{-HBpin})_2$ with cinnamaldehyde: Formation of $\text{P}^2$



After the reaction mentioned in section 4.2 (1 equiv of  $\text{Zn}(\text{L}^2)_2$  and 2 equiv of pinacolborane in  $\text{C}_6\text{D}_6$ ) became colorless and  $\text{Zn}(\text{L}^2\text{-HBpin})_2$  was formed, 2 equiv of cinnamaldehyde (21  $\mu\text{L}$ , 0.17 mmol) was added to the reaction mixture, resulting immediately in a very pale yellow solution. After 3 h the solvent was evaporated under vacuum and the residue was washed with hexane and filtered.  $^1\text{H}$  NMR of both solid and filtrate showed no hydroboration product, but the latter showed a new

product ( $\text{P}^2$ ). This benzothiazoline product was isolated using column chromatography and characterized by  $^1\text{H}$  and  $^{13}\text{C}$  NMR (Figures S15 and S16).

**$^1\text{H}$  NMR (300 MHz,  $\text{CDCl}_3$  at 25 °C):**  $\delta$  2.45 (s, 3H, S-Me), 4.40 (s, 2H, N- $\text{CH}_2$ ), 5.80 (dd, 1H, N-CHR-S), 6.26 (dd, 1H, Ar-H), 6.44 (m, 2H, Ar-H), 6.68 (td, 1H, Ar-H), 6.91 (td, 1H, Ar-H), 7.07 (dd, 1H, Ar-H), 7.14 (m, 1H, Ar-H), 7.30 (m, 7H, Ar-H).  **$^{13}\text{C}\{^1\text{H}\}$  NMR (75 MHz,  $\text{CDCl}_3$ , 25 °C,):** 15.1 (S-Me); 48.5 (N- $\text{CH}_2$ ); 73.1 (N-C-S); 107.8 (ArSNS-C); 118.9 (ArSNS-C); 121.8 (ArSNS-C); 125.0 (ArSNS-C); 125.0 (ArSNS-C); 125.6 (ArSNS-C); 125.7 (ArSNS-C); 126.89 (ArSNS-C); 127.0 (ArSNS-C); 127.4 (ArSNS-C); 127.8 (ArSNS-C); 128.2 (ArSNS-C); 128.6 (ArSNS-C); 129.6 (ArSNS-C); 132.3 (ArSNS-C); 135.8 (ArSNS-C); 137.0 (ArSNS-C); 146.8 ppm (ArSNS-C).

#### 4.5 Stoichiometric reaction of $\text{Zn}(\text{L}^1)(\text{L}^2)$ with benzaldehyde and HBpin

In order to find out which one of  $\text{L}^1$  and  $\text{L}^2$  plays the dominant role in catalysis, an orange suspension of  $\text{Zn}(\text{L}^1)(\text{L}^2)$  (0.01 g, 0.02 mmol) in  $\text{C}_6\text{D}_6$  was charged with benzaldehyde (3.5  $\mu\text{L}$ , 0.03 mmol), and then pinacolborane (2.5  $\mu\text{L}$ , 0.02 mmol) was added, giving a homogeneous light orange solution after 3-5 min. The crude  $^1\text{H}$  NMR spectrum showed free benzaldehyde, hydroborated benzaldehyde, N-borylated  $\text{L}^1$  and  $\text{P}^1$ . After addition of the second equivalent of pinacolborane, the  $^1\text{H}$ -NMR spectrum showed hydroborated benzaldehyde, N-borylated  $\text{L}^1$  and  $\text{P}^1$  (Figure S26).

## 5. NMR and EI-MS Spectra

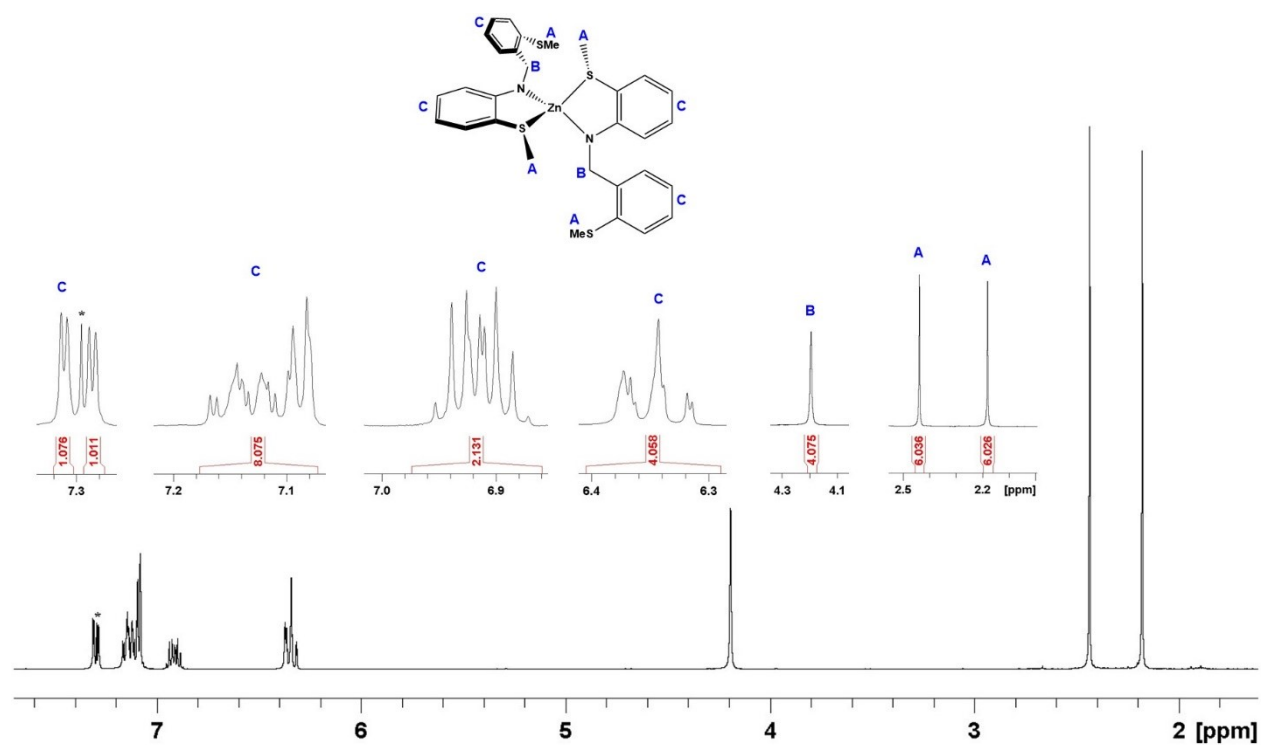


**Figure S1.**  $^1H$  NMR spectrum (300 MHz) of  $Zn(L^1)_2$ . \* indicates protic impurity in  $C_6D_6$ .

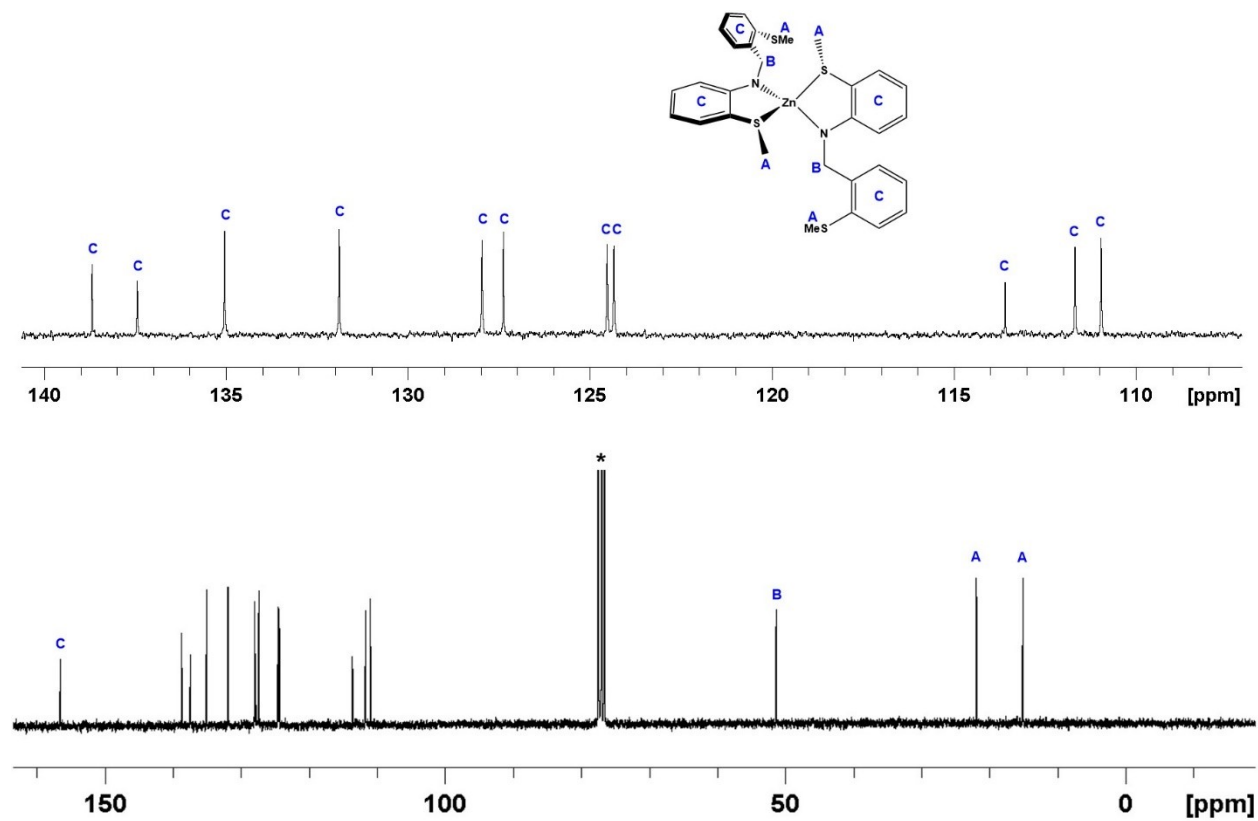


**Figure S2.**  $^{13}C\{^1H\}$  NMR spectrum (75 MHz) of  $Zn(L^1)_2$ . \* indicates protic impurity in  $C_6D_6$ .

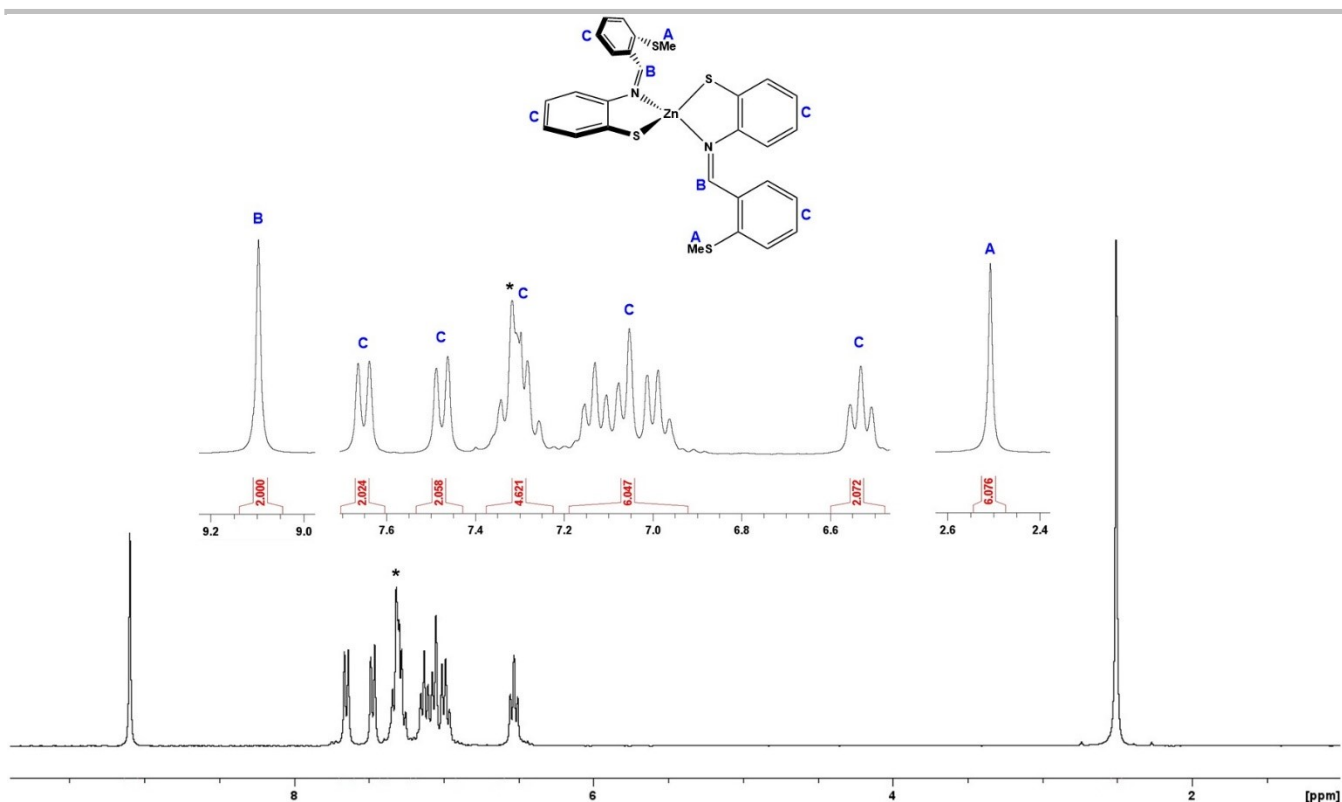


**Figure S3.**  $^1\text{H}$  NMR spectrum (300 MHz) of  $\text{Zn}(\text{L}^2)_2$ . \* indicates protic impurity in  $\text{CDCl}_3$ .

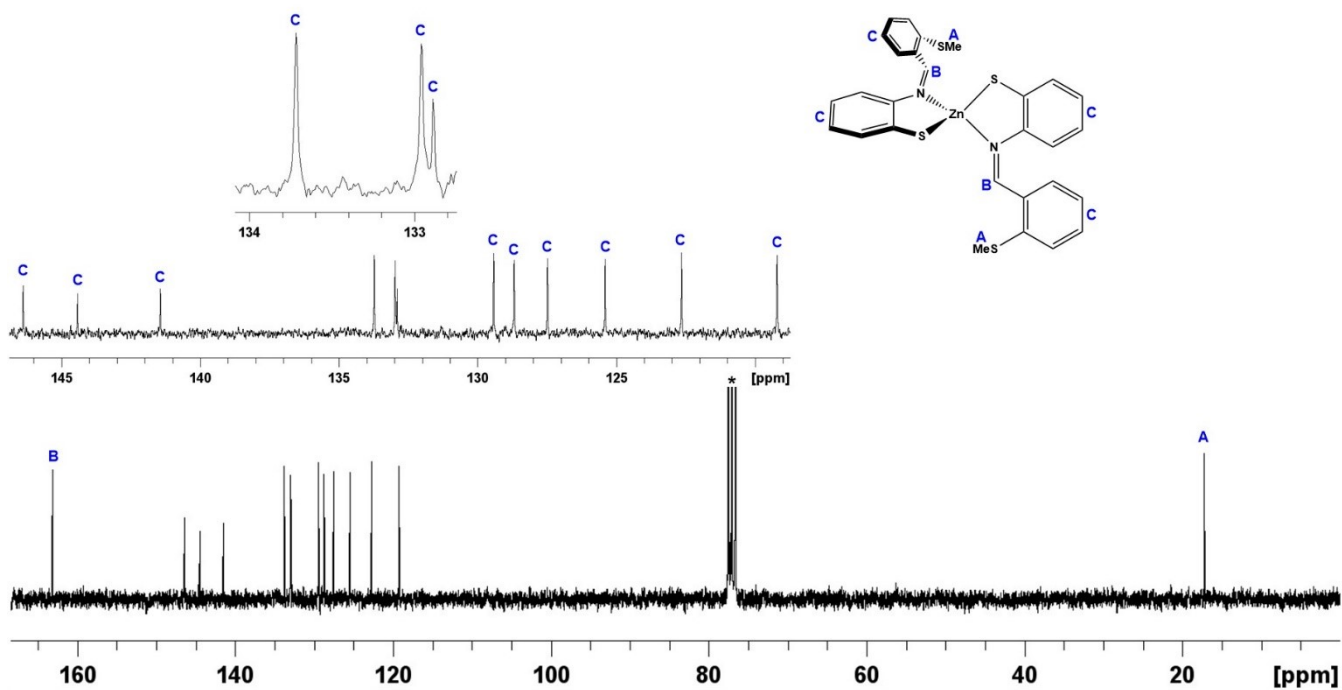


**Figure S4.**  $^{13}\text{C}\{^1\text{H}\}$  NMR spectrum (75 MHz) of  $\text{Zn}(\text{L}^2)_2$ . \* indicates protic impurity in  $\text{CDCl}_3$ .

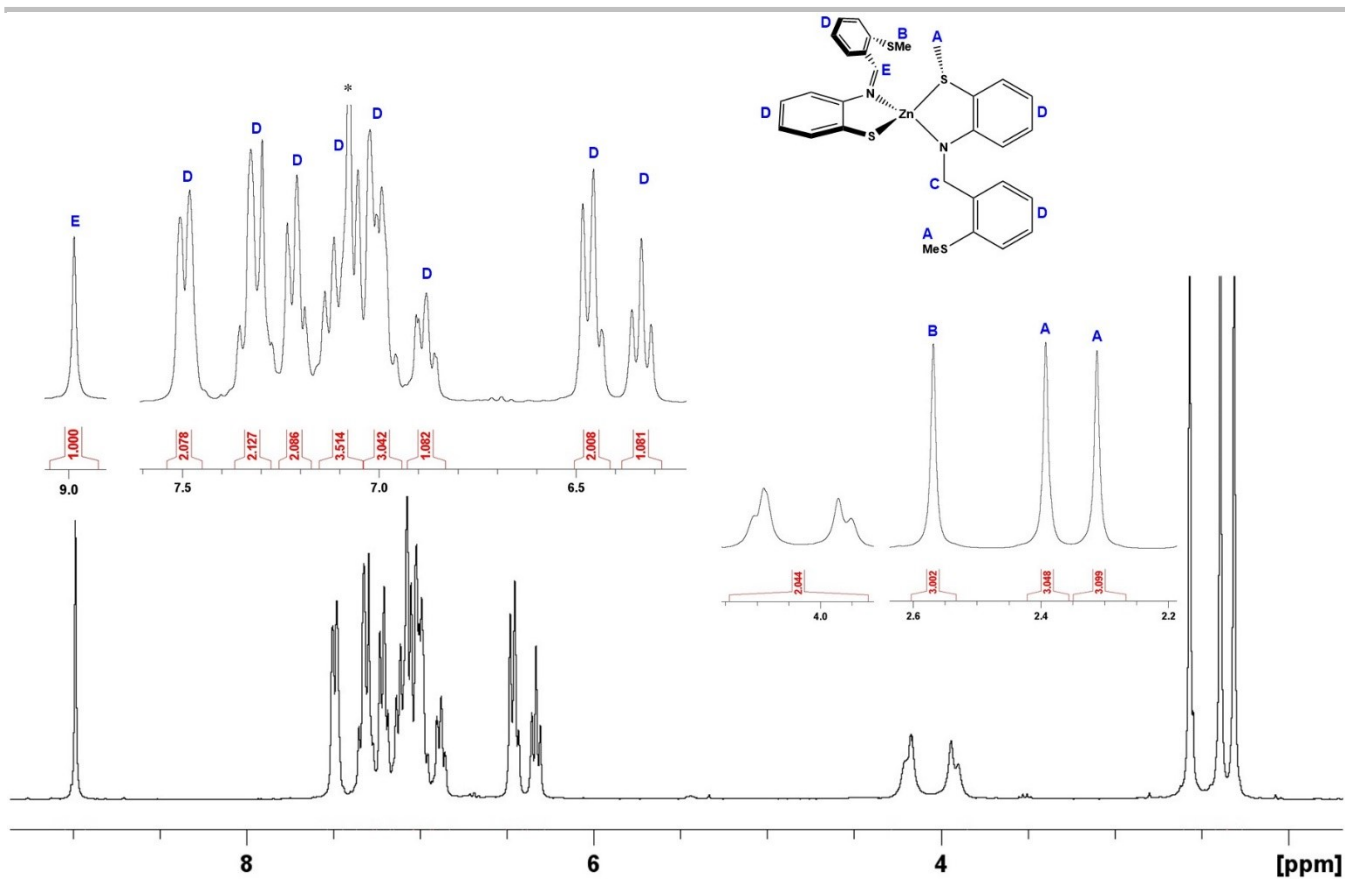


**Figure S5.**  $^1\text{H}$  NMR spectrum (300 MHz) of  $\text{Zn}(\text{L}^1)(\text{L}^2)$ . \* indicates protic impurity in  $\text{CDCl}_3$ .

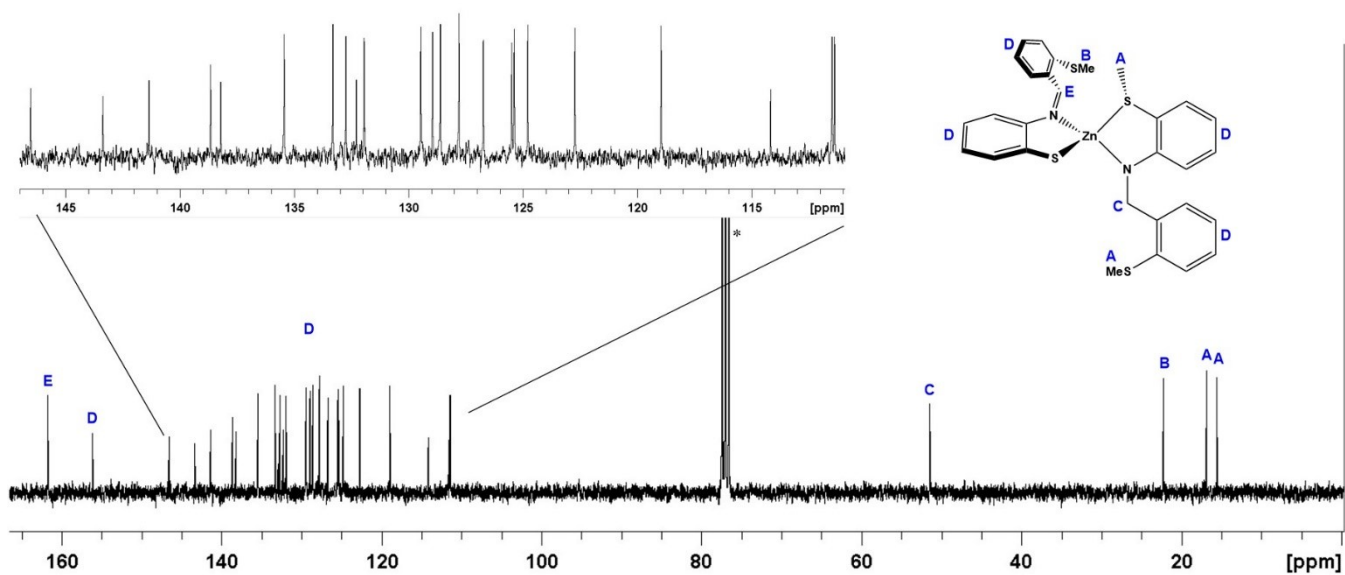


**Figure S6.**  $^{13}\text{C}\{^1\text{H}\}$  NMR spectrum (75 MHz) of  $\text{Zn}(\text{L}^1)(\text{L}^2)$ . \* indicates protic impurity in  $\text{CDCl}_3$ .

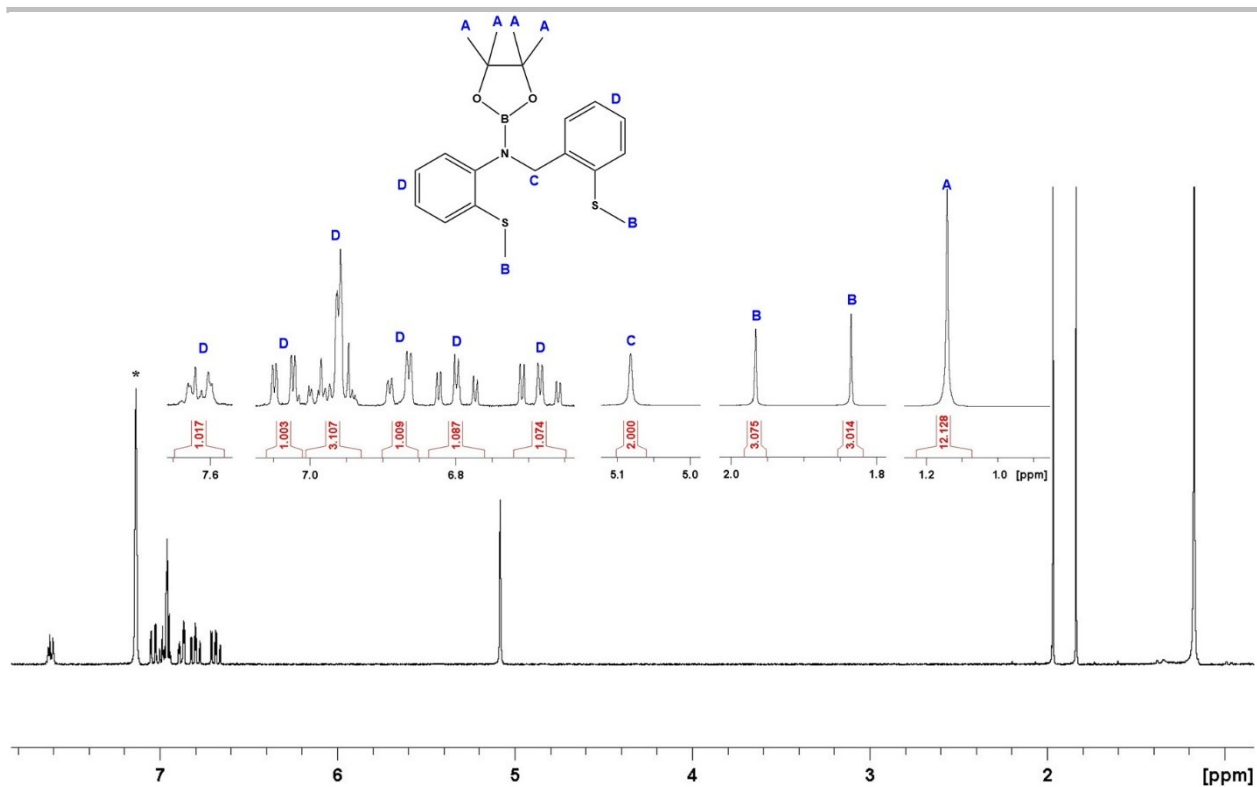


Figure S7.  $^1\text{H}$  NMR spectrum (300 MHz) of N-borylated L<sup>1</sup>. \* indicates protic impurity in  $\text{C}_6\text{D}_6$ .

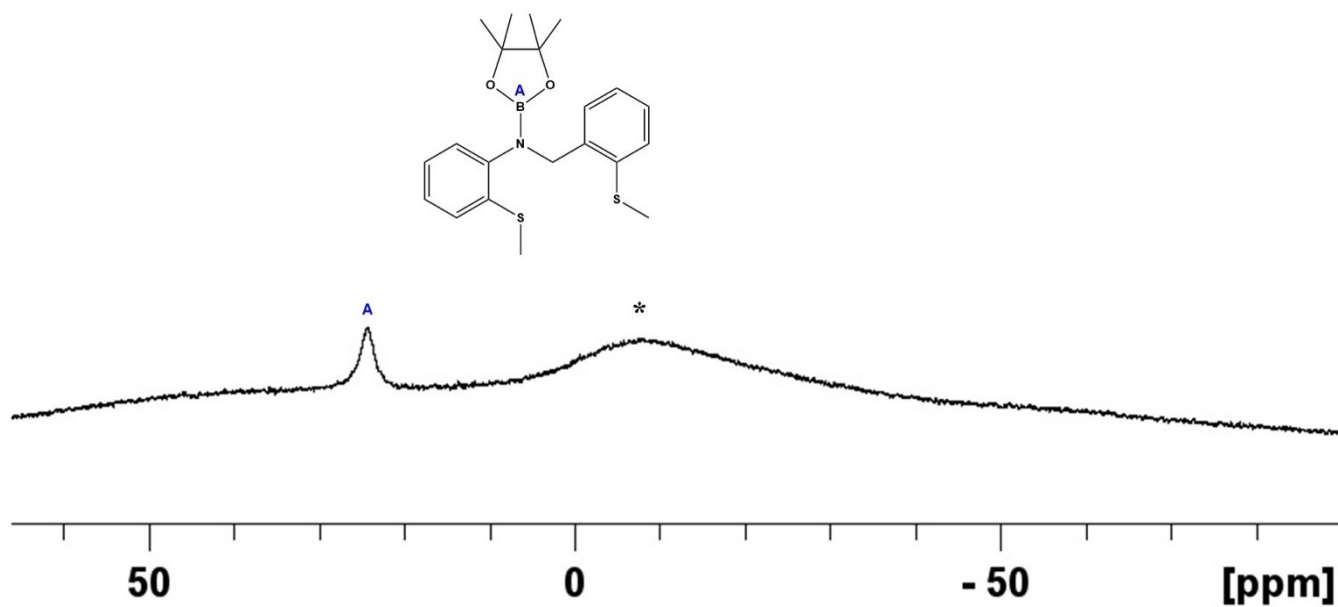
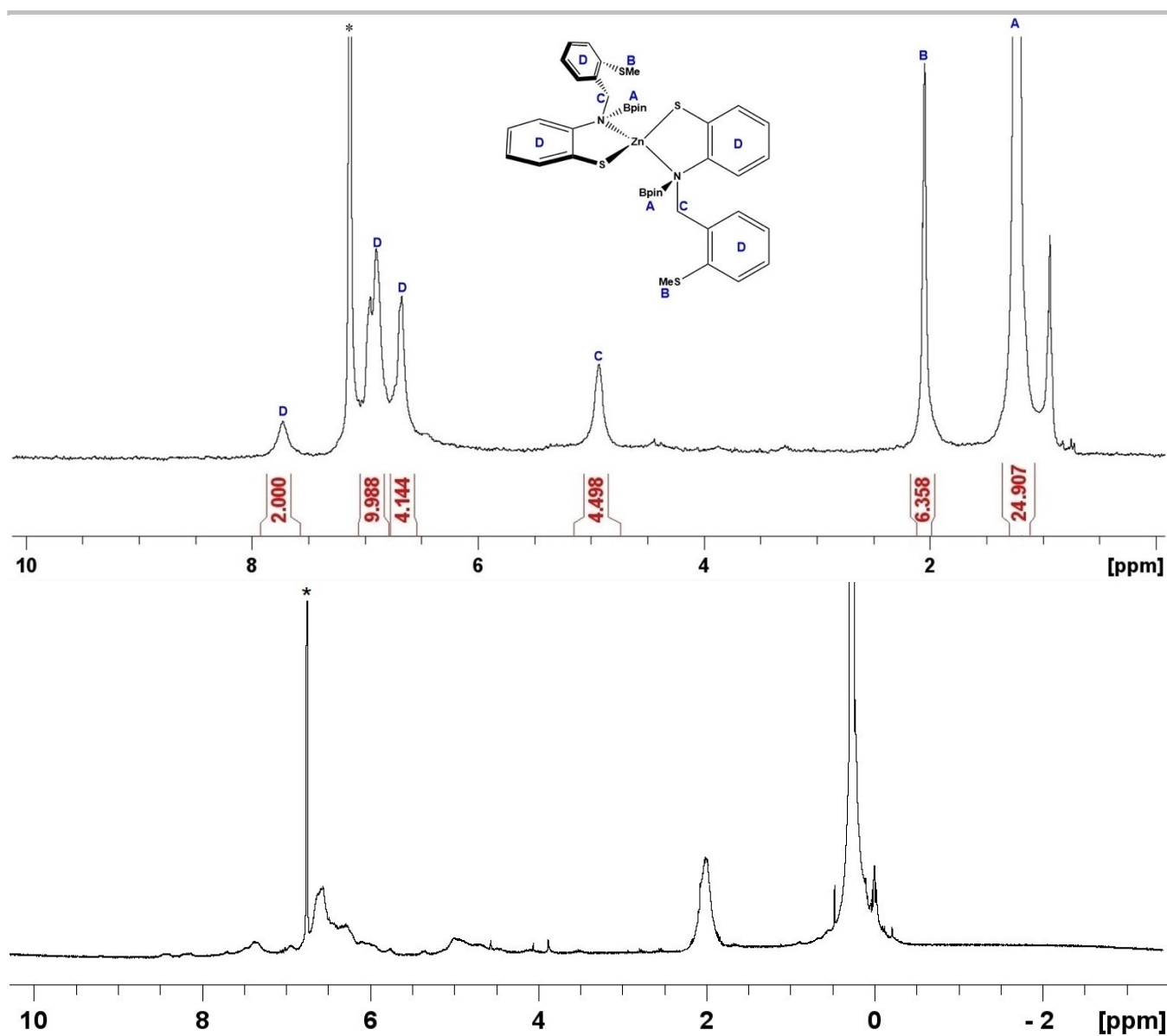
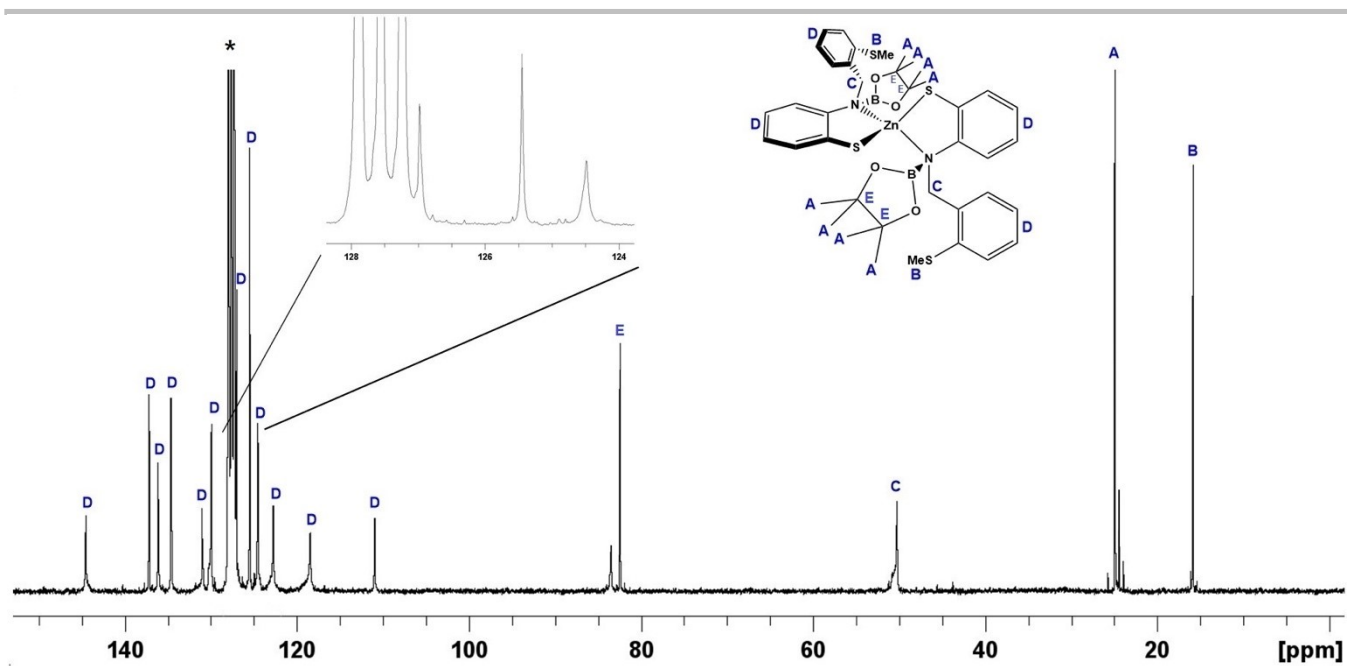


Figure S8.  $^{11}\text{B}\{^1\text{H}\}$  NMR spectrum (96 MHz) of N-borylated L<sup>1</sup>. \* indicates boron in probe.



**Figure S9.**  $^1\text{H}$  NMR spectra (300 MHz,  $45^\circ\text{C}$  top, room temperature bottom) of  $\text{Zn}(\text{L}^2\text{-HBpin})_2$  \* indicates protic impurity in  $\text{C}_6\text{D}_6$ .



**Figure S10.**  $^{13}\text{C}\{^1\text{H}\}$  NMR spectrum (75 MHz, 45°C) of  $\text{Zn}(\text{L}^2\text{-HBpin})_2$  \* indicates protic impurity in  $\text{C}_6\text{D}_6$ .

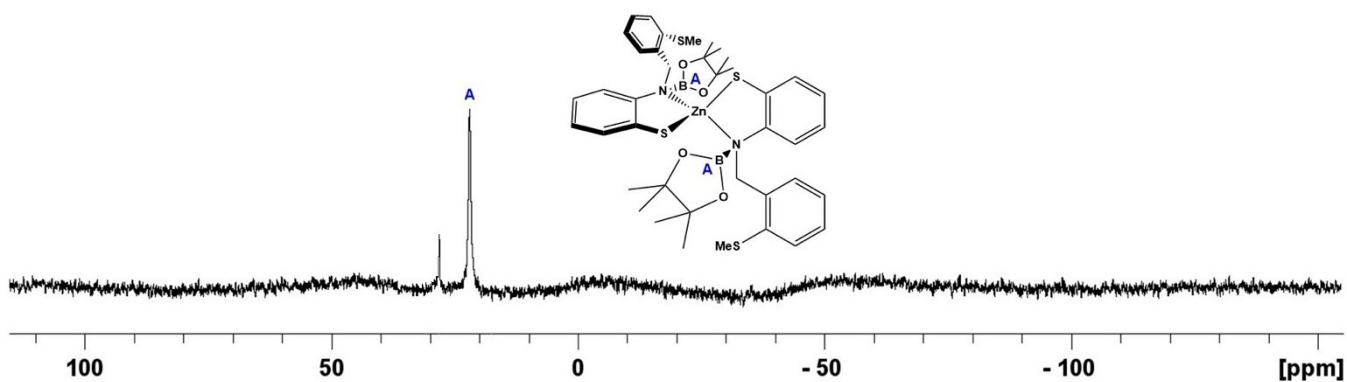


**Figure S11.**  $^{11}\text{B}\{^1\text{H}\}$  NMR spectrum (96 MHz, 45°C) of  $\text{Zn}(\text{L}^2\text{-HBpin})_2$ .

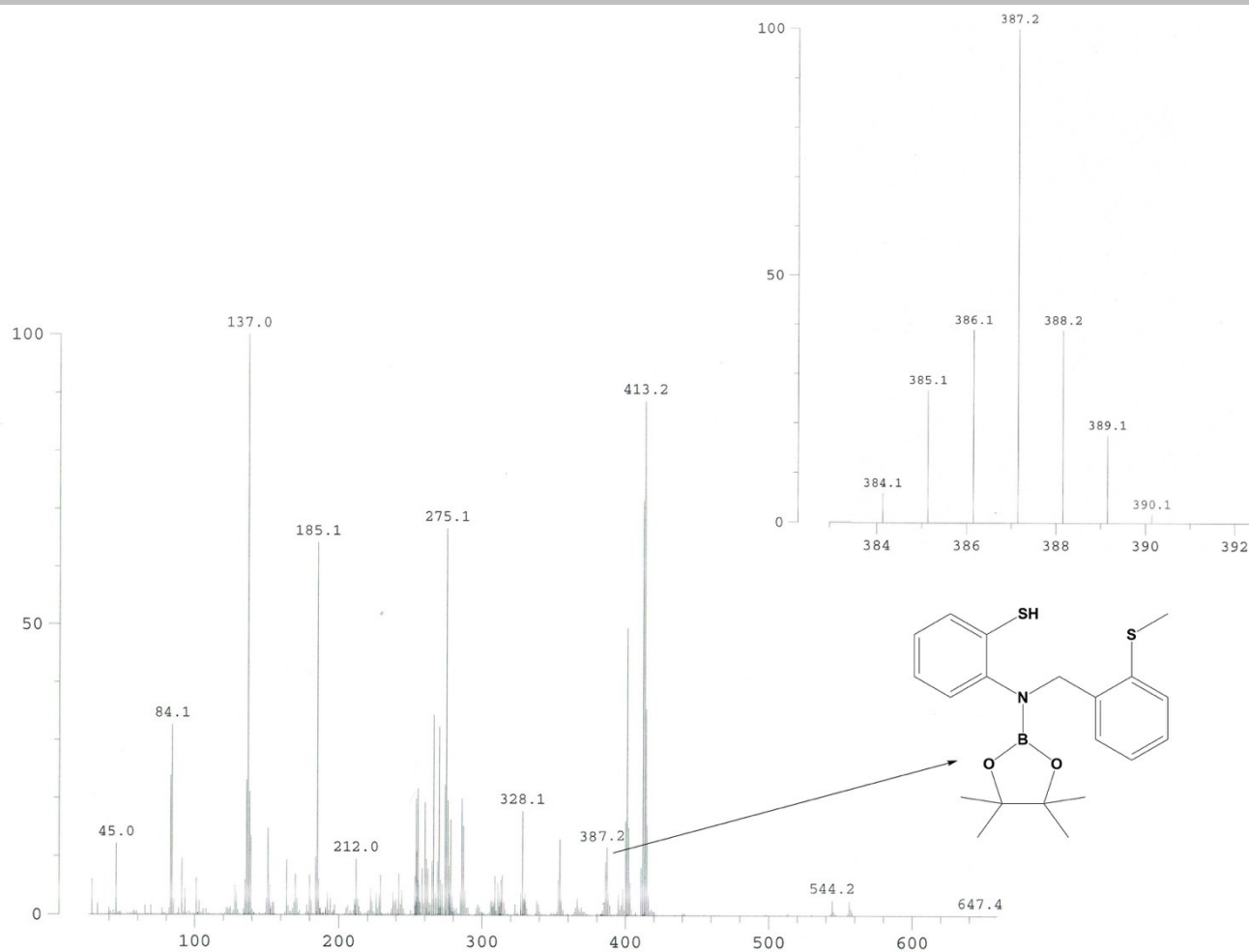


Figure S12. EI-MS spectrum of  $\text{Zn}(\text{L}^2\text{-HBpin})_2$  showing  $[\text{L}^2\text{-HBpin}]^+$

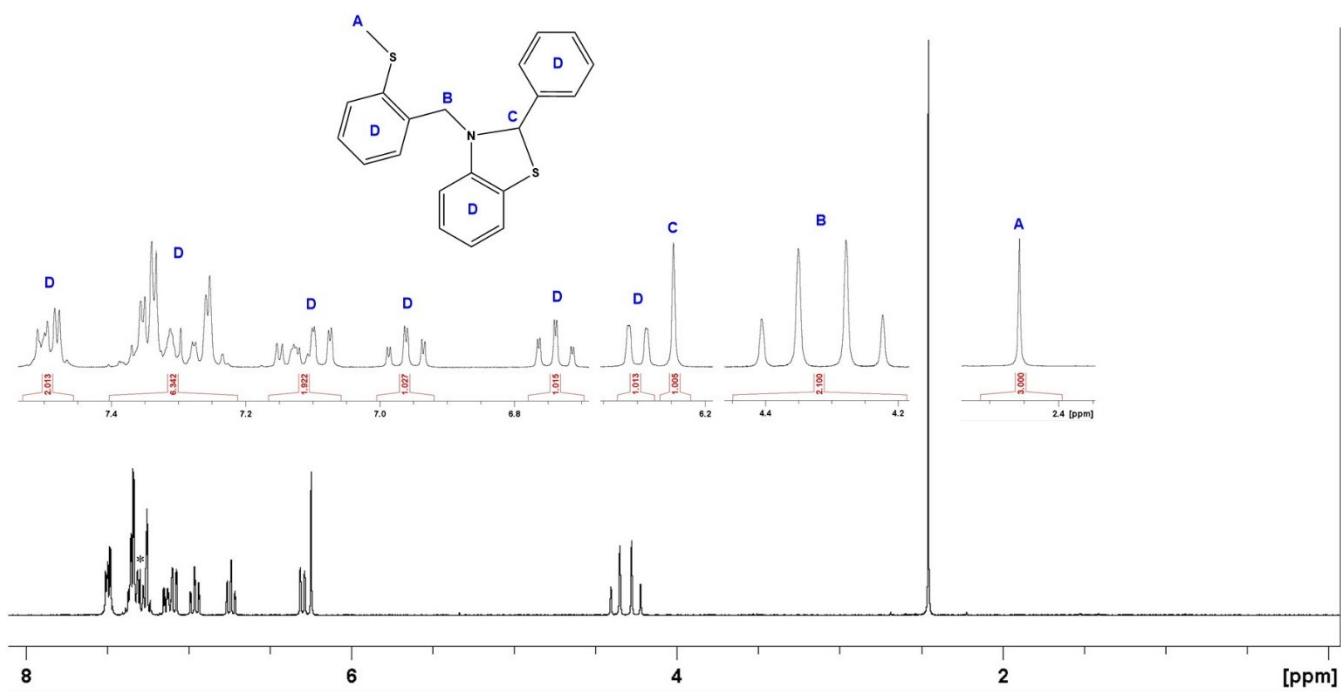
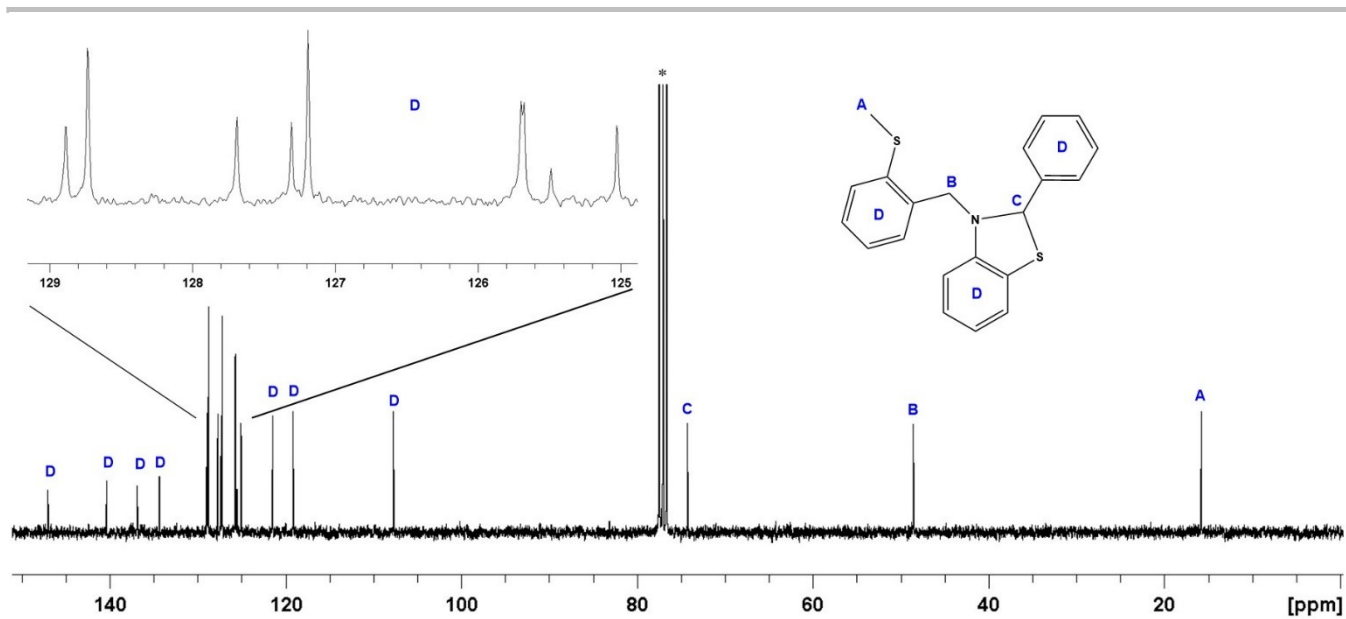
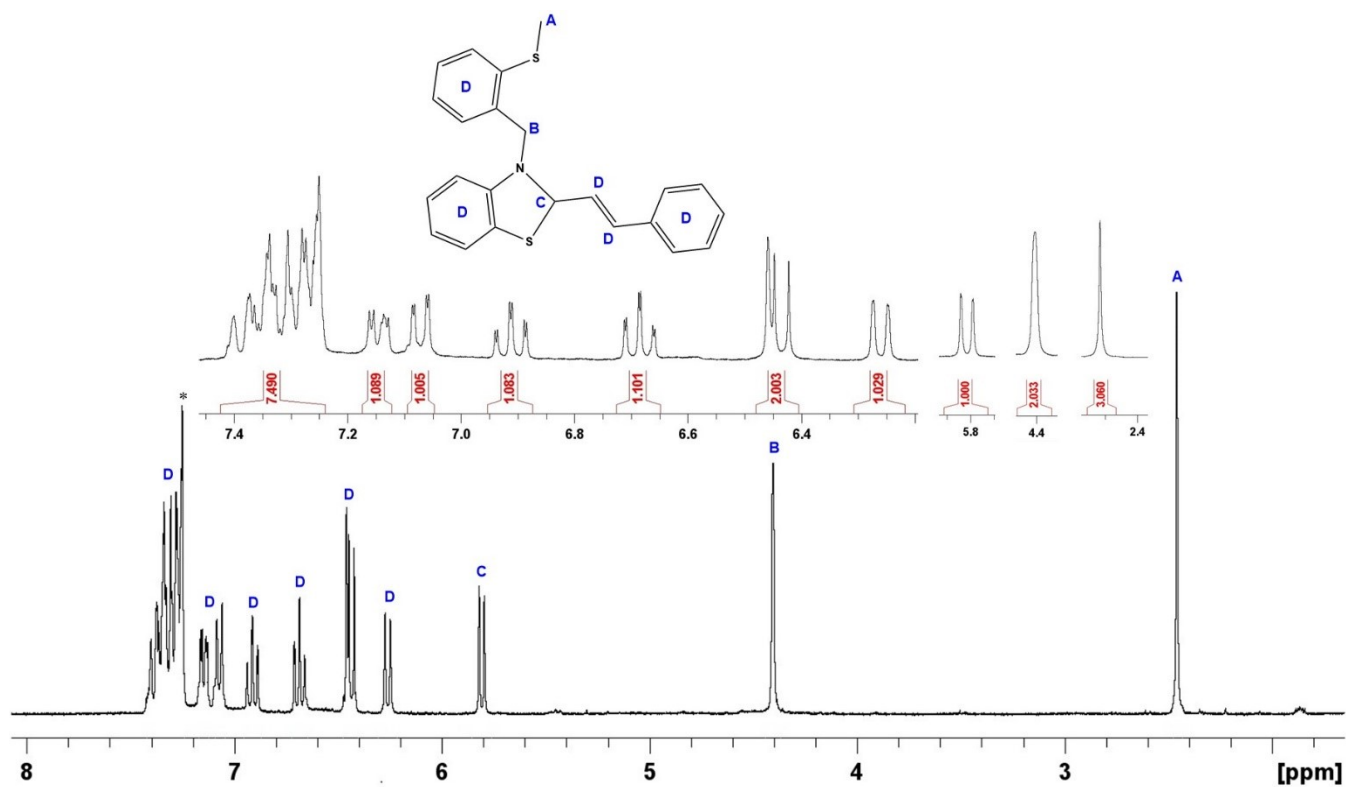


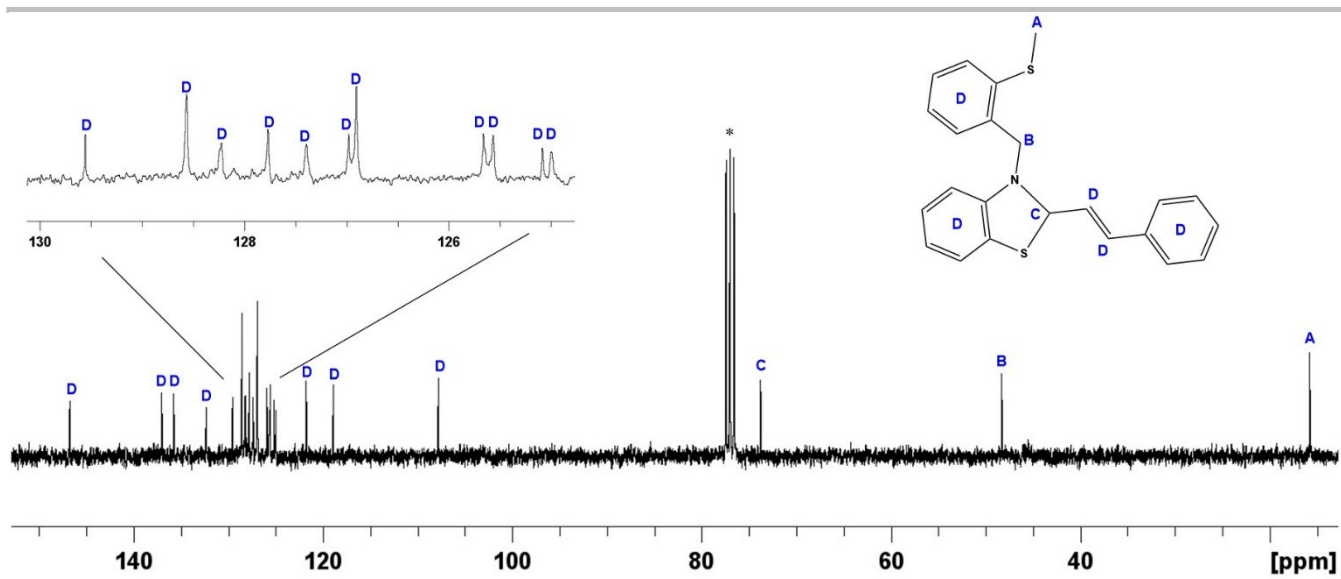
Figure S13.  $^1\text{H}$  NMR spectrum (300 MHz) of  $\text{P}^1$ . \* indicates protic impurity in  $\text{CDCl}_3$ .



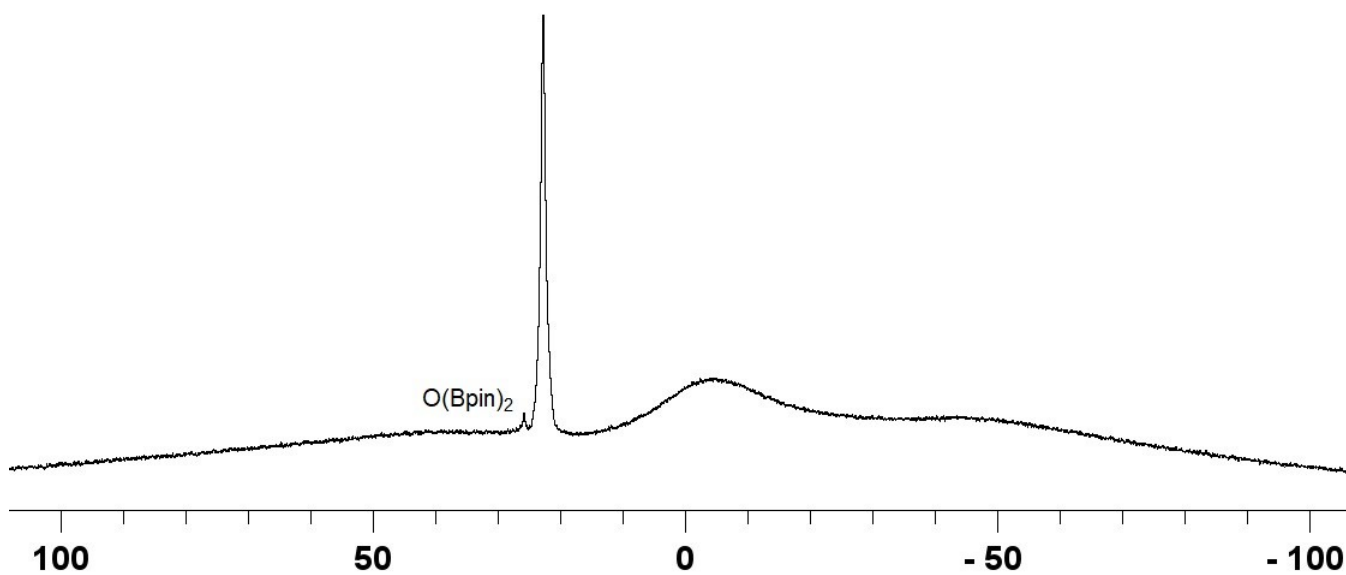
**Figure S14.**  $^{13}\text{C}\{^1\text{H}\}$  NMR spectrum (75 Mz) of  $\text{P}^1$ . \* indicates protic impurity in  $\text{CDCl}_3$ .



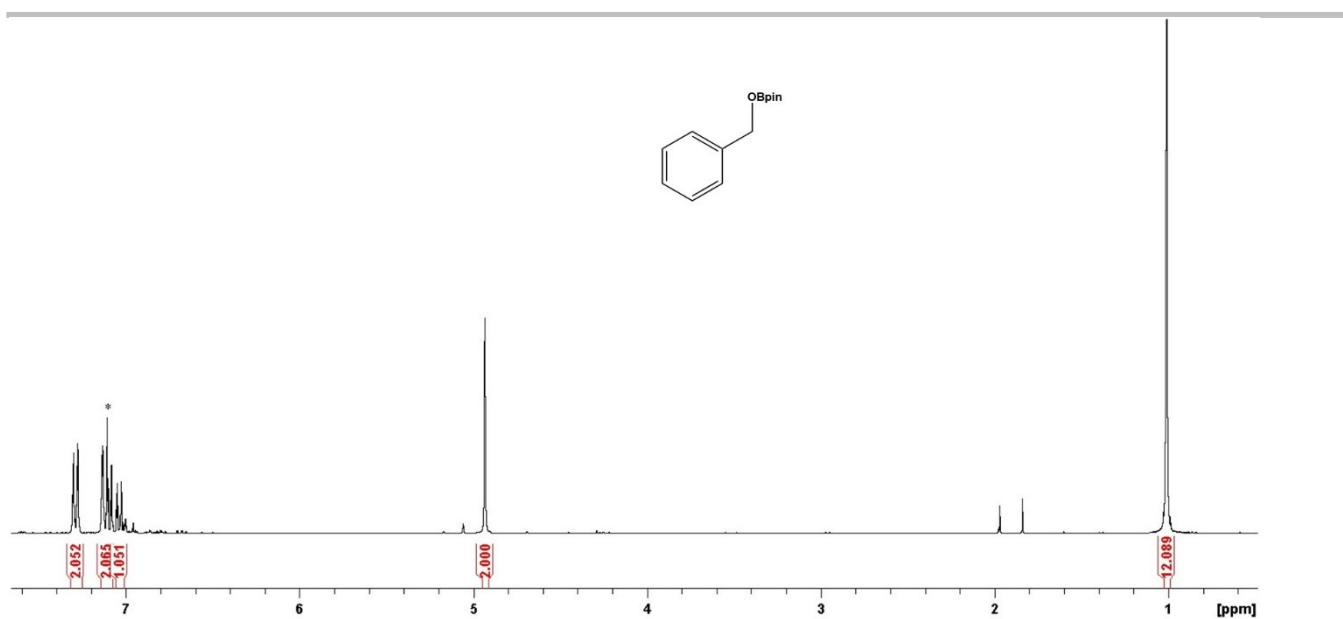
**Figure S15.**  $^1\text{H}$  NMR spectrum (300 MHz) of  $\text{P}^2$ . \* indicates protic impurity in  $\text{CDCl}_3$ .



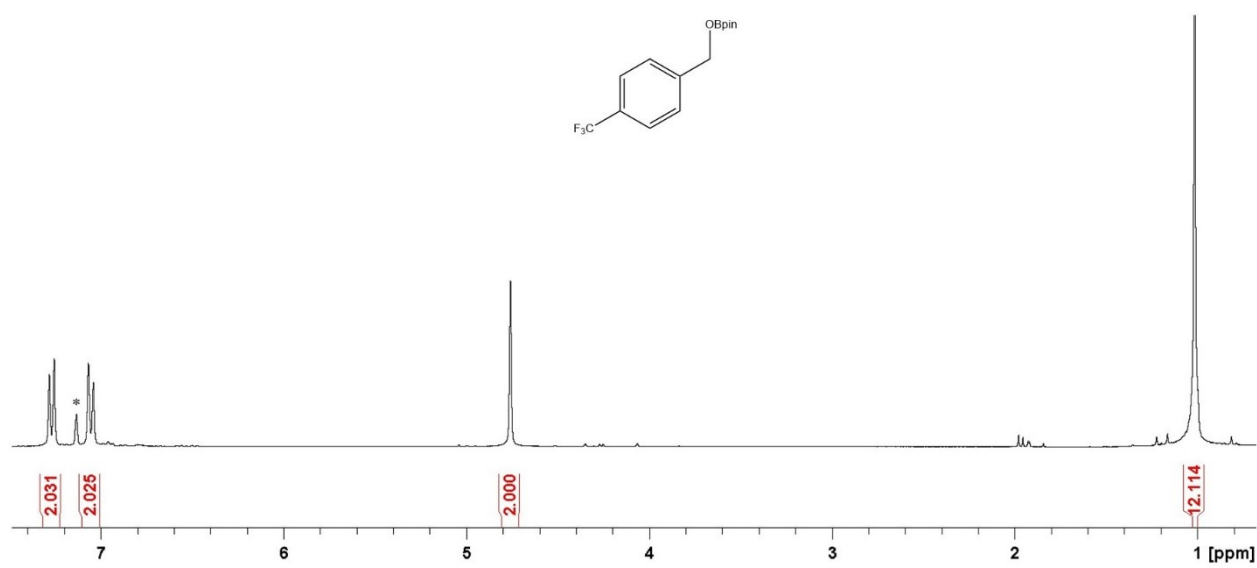
**Figure S16.**  $^{13}\text{C}\{^1\text{H}\}$  NMR spectrum (75 MHz) of  $\text{P}^2$ . \* indicates protic impurity in  $\text{CDCl}_3$ .



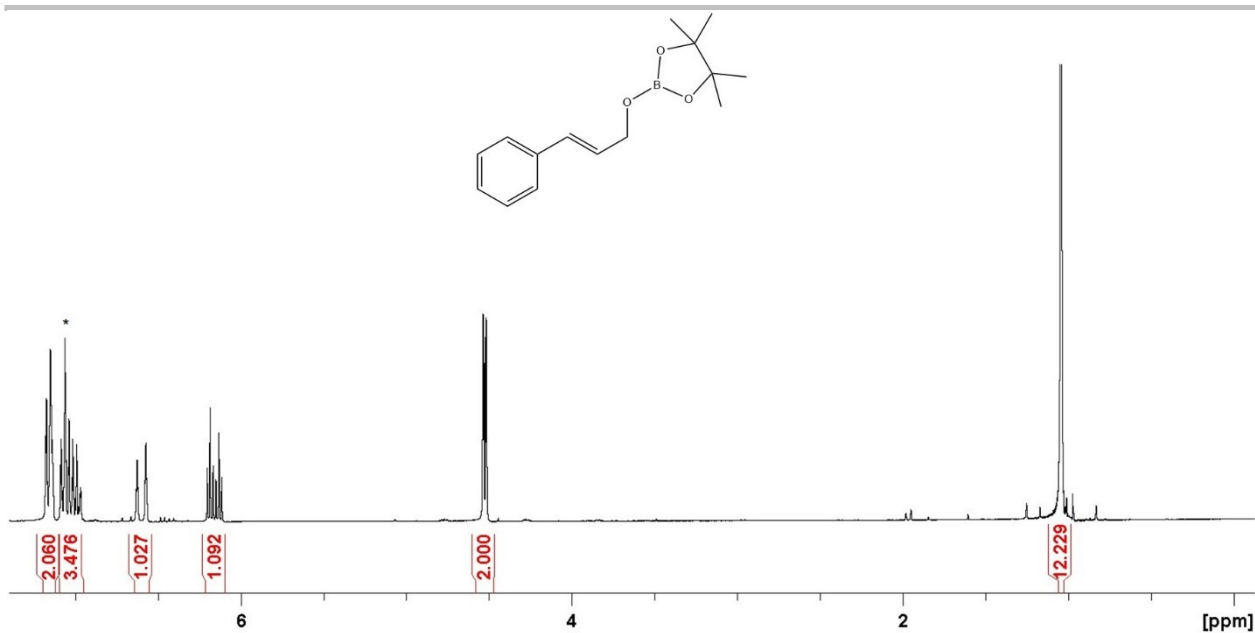
**Figure S17.**  $^{11}\text{B}$  NMR spectrum (96 MHz) of  $\text{Zn}(\text{L}^2)_2$ -catalyzed hydroboration mixture showing  $\text{O}(\text{Bpin})_2$ .



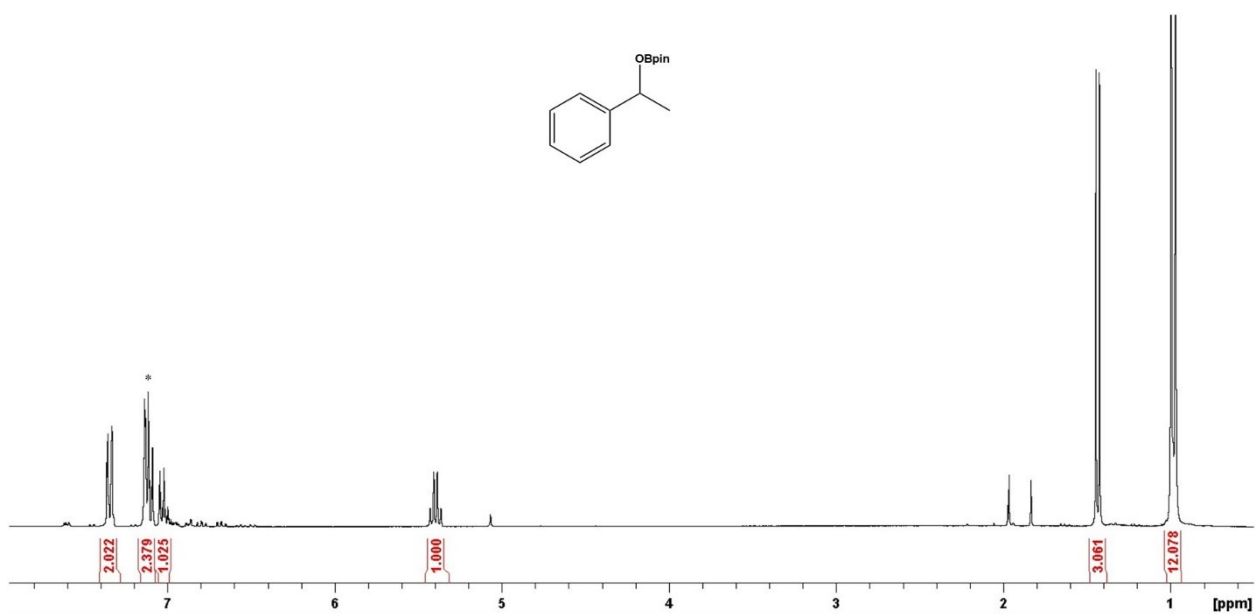
**Figure S18.**  $^1\text{H}$  NMR spectrum (300 MHz) of benzaldehyde hydroboration product. \* indicates protic impurity in  $\text{C}_6\text{D}_6$ .



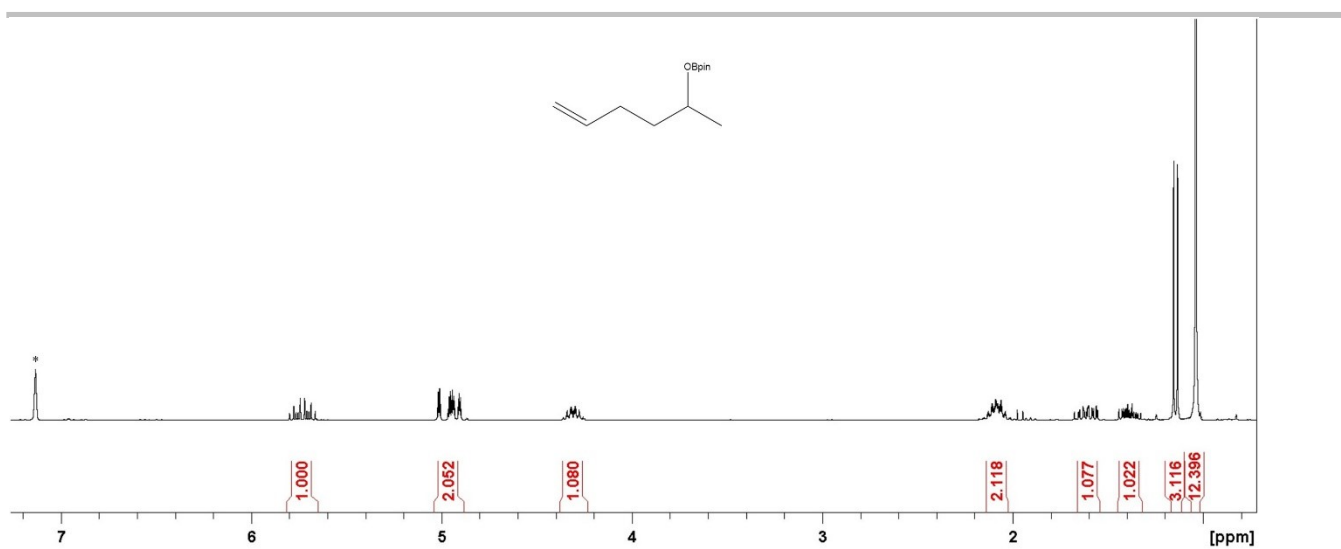
**Figure S19.**  $^1\text{H}$  NMR spectrum (300 MHz) of 4-trifluoromethylbenzaldehyde hydroboration product. \* indicates protic impurity in  $\text{C}_6\text{D}_6$ .



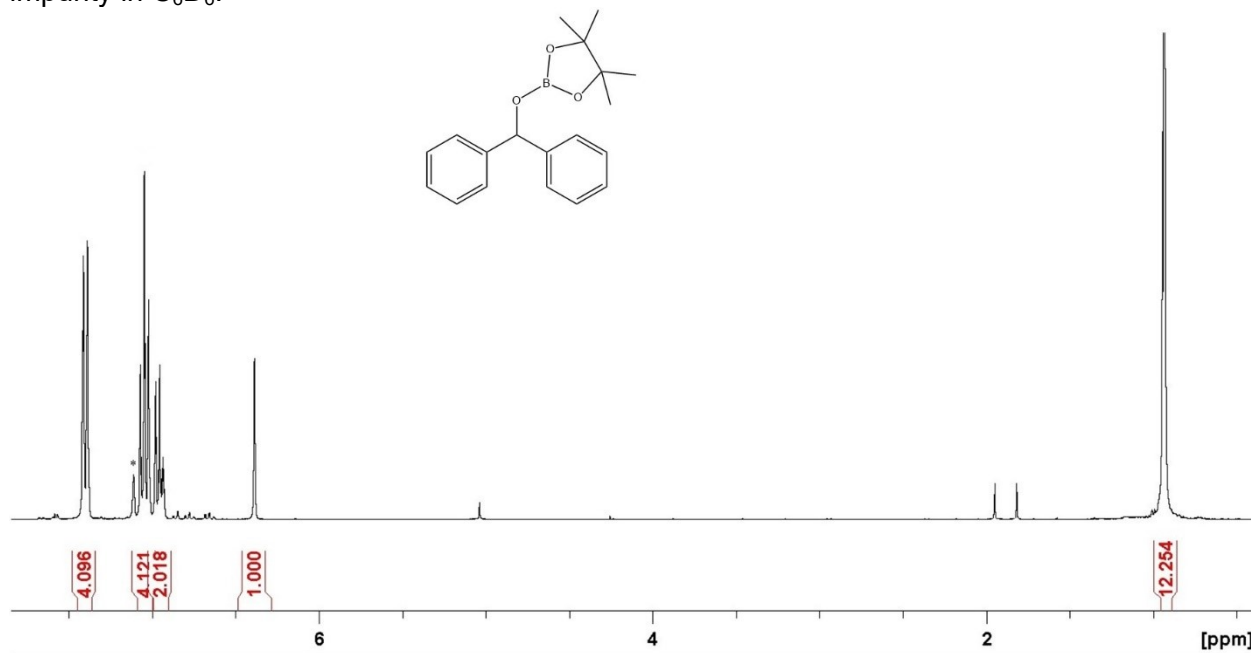
**Figure S20.**  $^1\text{H}$  NMR spectrum (300 MHz) of cinnamaldehyde hydroboration product. \* indicates protic impurity in  $\text{C}_6\text{D}_6$



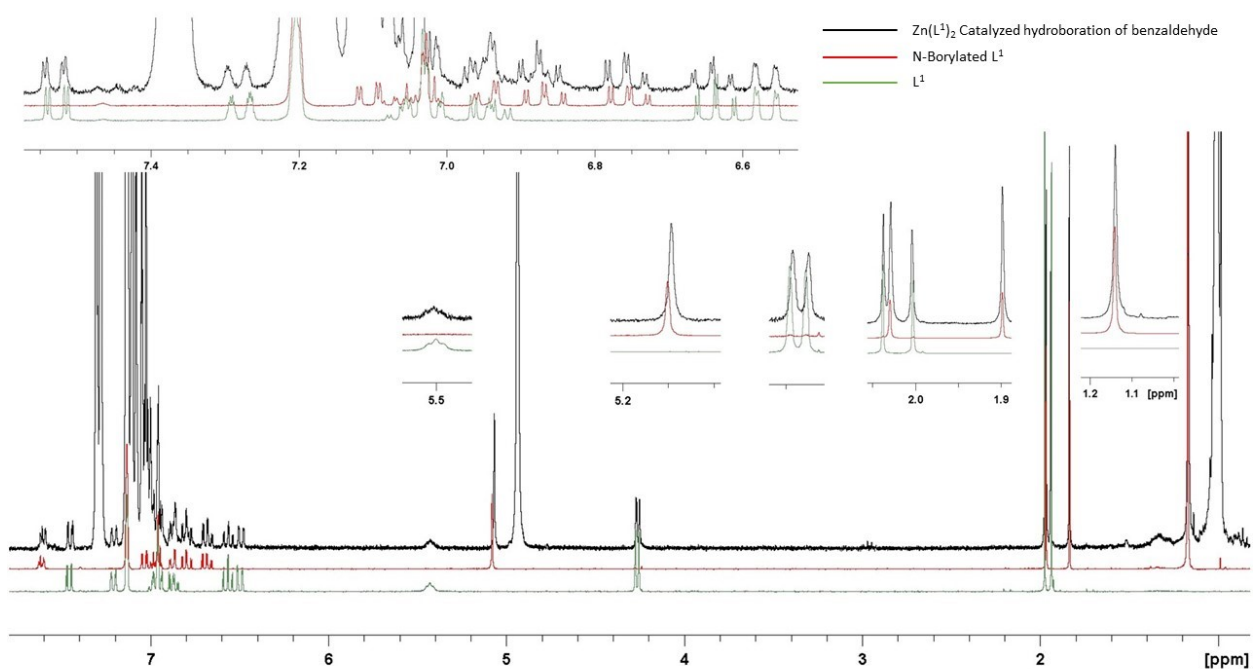
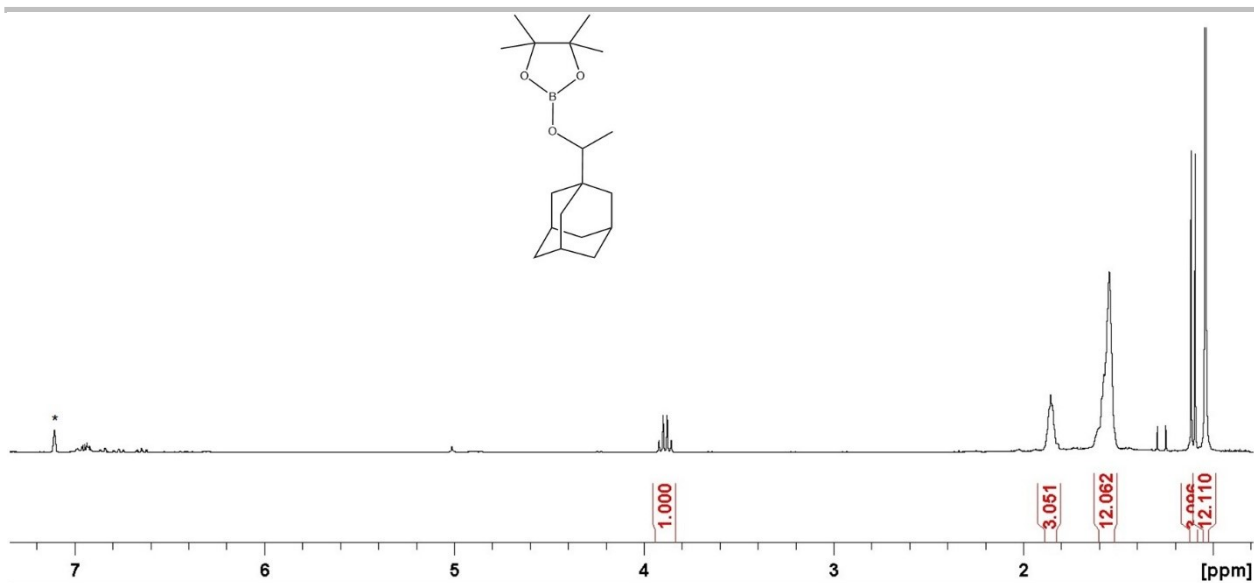
**Figure S21.**  $^1\text{H}$  NMR spectrum (300 MHz) of acetophenone hydroboration product. \* indicates protic impurity in  $\text{C}_6\text{D}_6$ .



**Figure S22.**  $^1\text{H}$  NMR spectrum (300 MHz) of benzophenone hydroboration product. \* indicates protic impurity in  $\text{C}_6\text{D}_6$ .



**Figure S23.**  $^1\text{H}$  NMR spectrum (300 MHz) of 5-hexen-2-one hydroboration product. \* indicates protic impurity in  $\text{C}_6\text{D}_6$ .



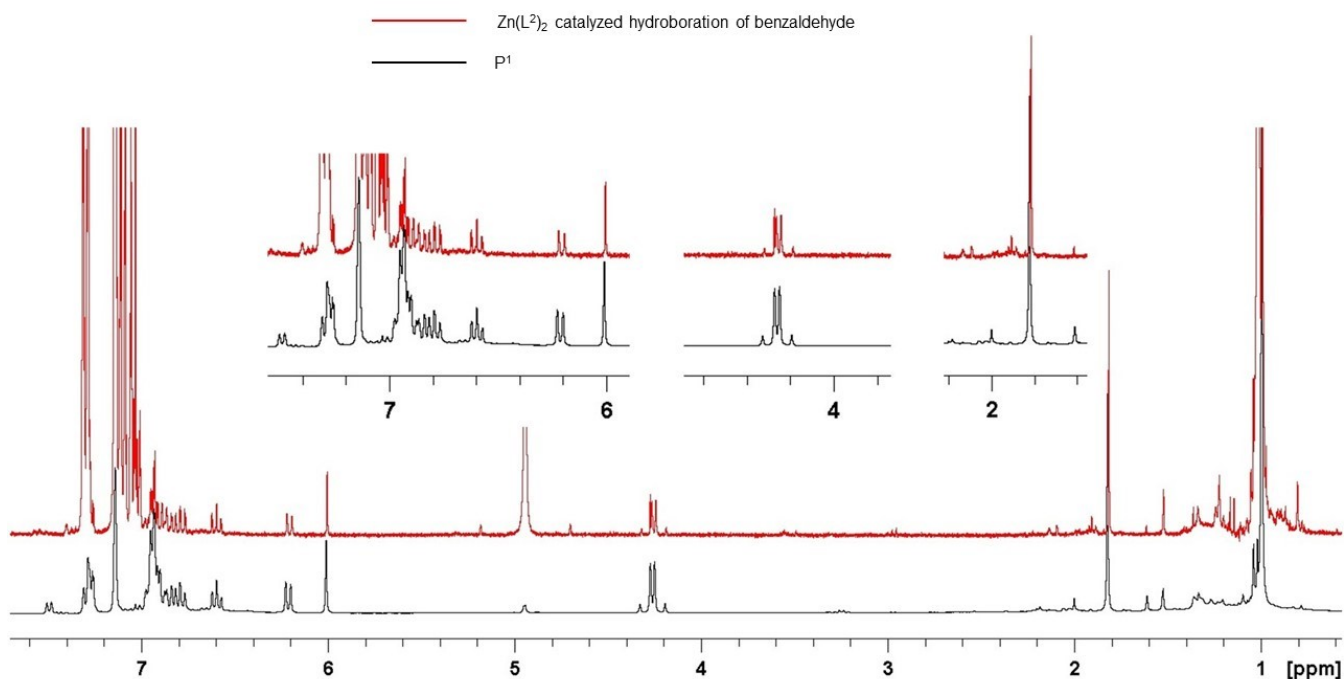


**Figure S26.**  $^1\text{H}$  NMR spectra (300 MHz,  $\text{C}_6\text{D}_6$ ) of  $\text{P}^1$  and  $\text{Zn}(\text{L}^2)_2$  in catalytic benzaldehyde hydroboration.

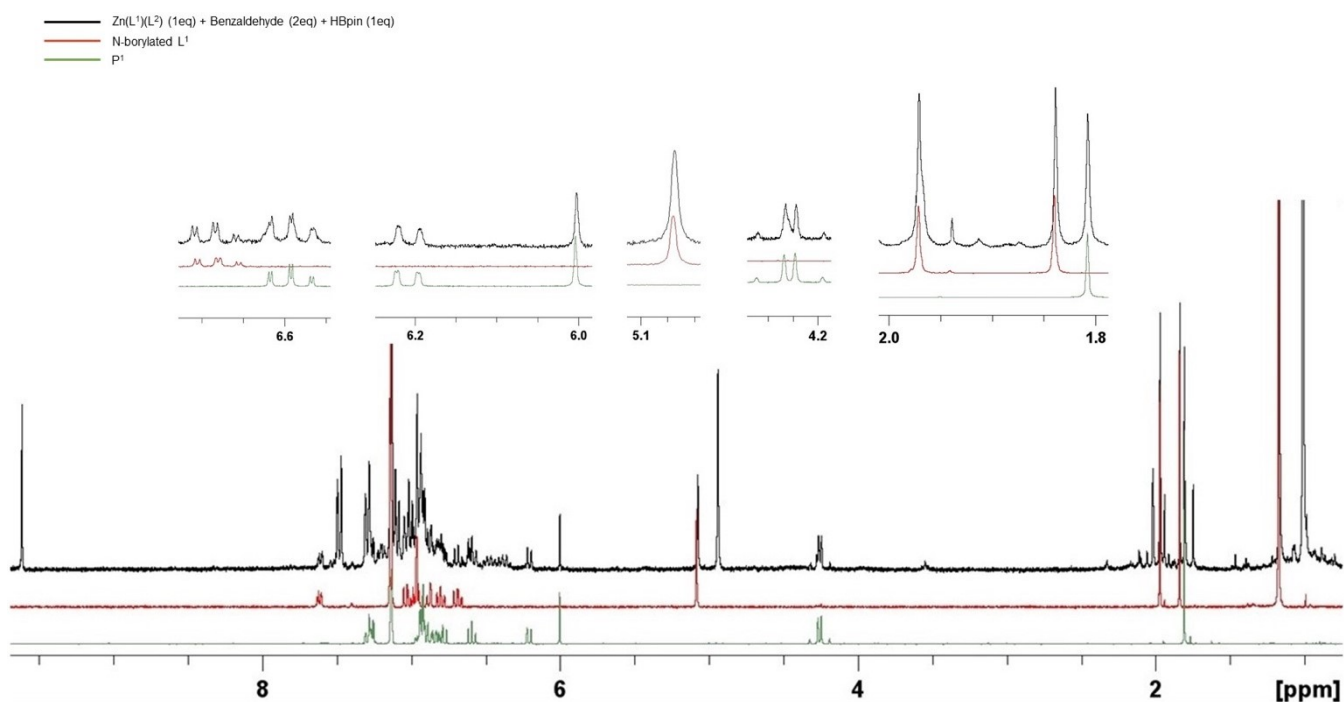


**Figure S27.**  $^1\text{H}$  NMR spectra (300 MHz) of  $\text{P}^1$ , and N-borylated  $\text{L}^1$ , and stoichiometric reaction of  $\text{Zn}(\text{L}^1)(\text{L}^2)$  with benzaldehyde (2eq) and HBpin (1eq) in  $\text{C}_6\text{D}_6$ .

## 6. Monitoring Acetophenone Hydroboration Reactions Using Zinc Complexes

To monitor the reaction progress, a vial was charged with acetophenone (116  $\mu\text{L}$ , 1.00 mmol) and either  $\text{Zn}(\text{L}^1)_2$  (6.1 mg, 1 mol%),  $\text{Zn}(\text{L}^2)_2$  (5.8 mg, 1 mol%), or  $\text{Zn}(\text{L}^1)(\text{L}^2)$  (5.9 mg, 1 mol%), or 0.5 mL of stock solution of  $\text{Zn}(\text{L}^1)(\text{L}^2)$  (0.59 mg, 0.1 mol%), then 0.3 mL of  $\text{C}_6\text{D}_6$  was added and the solution transferred to an NMR tube and capped with a rubber septum. Another vial was charged with pinacolborane (144.5  $\mu\text{L}$ , 1.00 mmol) and 0.3 mL  $\text{C}_6\text{D}_6$ , and the solution was transferred to a 1 mL syringe. Then, the syringe was capped by poking into the rubber septum. The NMR tube containing the reaction mixture and the syringe were removed from the glovebox. The HBpin was injected into the NMR tube, shaken quickly, and immediately inserted into the NMR spectrometer. A  $^1\text{H}$  NMR spectrum was taken every 15-25 sec for 25 min at room temperature. Concentration of the product was calculated based on the characteristic signals of the product and acetophenone.

For the reactions carried out in THF, the conditions and procedures are the same but the solvent was THF instead of  $\text{C}_6\text{D}_6$ , and the concentration of the product was calculated based on the characteristic signals of the product and HBpin by  $^{11}\text{B}$  NMR.

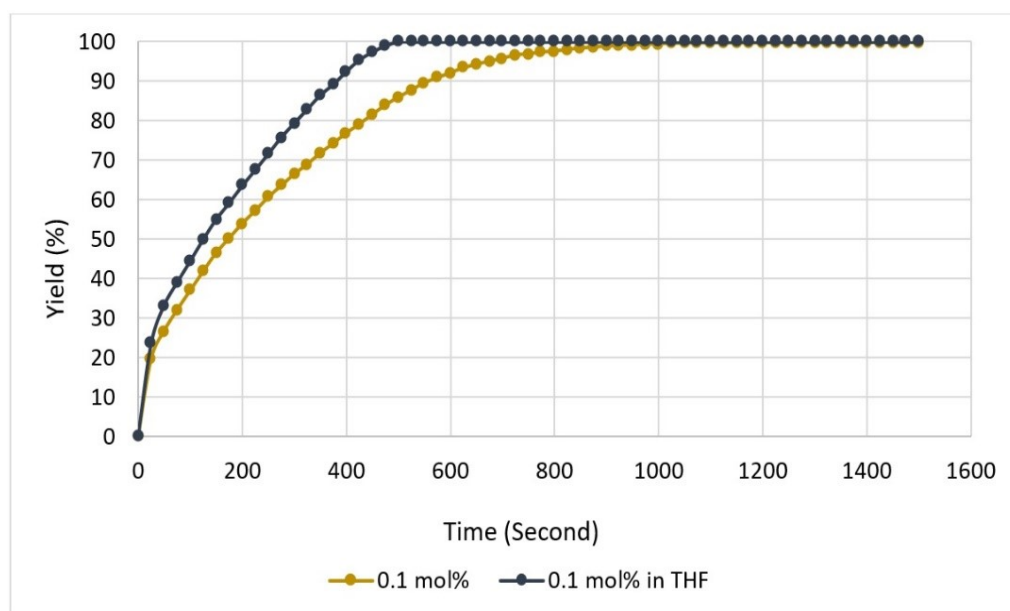


**Figure S28.** Profiles of acetophenone hydroboration using HBpin catalyzed by  $\text{Zn}(\text{L}^1)(\text{L}^2)$  with 0.1 mol% loading in  $\text{C}_6\text{D}_6$  and THF.

### Isolation of Zn alkoxide using bipyridine ligand

To a vial containing a solution of acetophenone (1160  $\mu\text{L}$ , 10.00 mmol) and  $\text{Zn}(\text{L}^1)_2$  (61 mg, 1 mol%) or  $\text{Zn}(\text{L}^2)_2$  (58 mg, 1 mol%), in 2 mL of benzene was added pinacolborane (1445  $\mu\text{L}$ , 10.00 mmol) and the mixture stirred for 40 mins in room temperature. Then, 15 mg of bipy (15 0.1 mmol) was added and the final mixture stirred for 2h. Afterward, the solvent was evaporated under vacuum and EI-MS analysis was performed, but no  $(\text{Bipy})\text{Zn}(\text{alkoxide})_2$  was detected.

## 7. EI-MS spectra of complexes

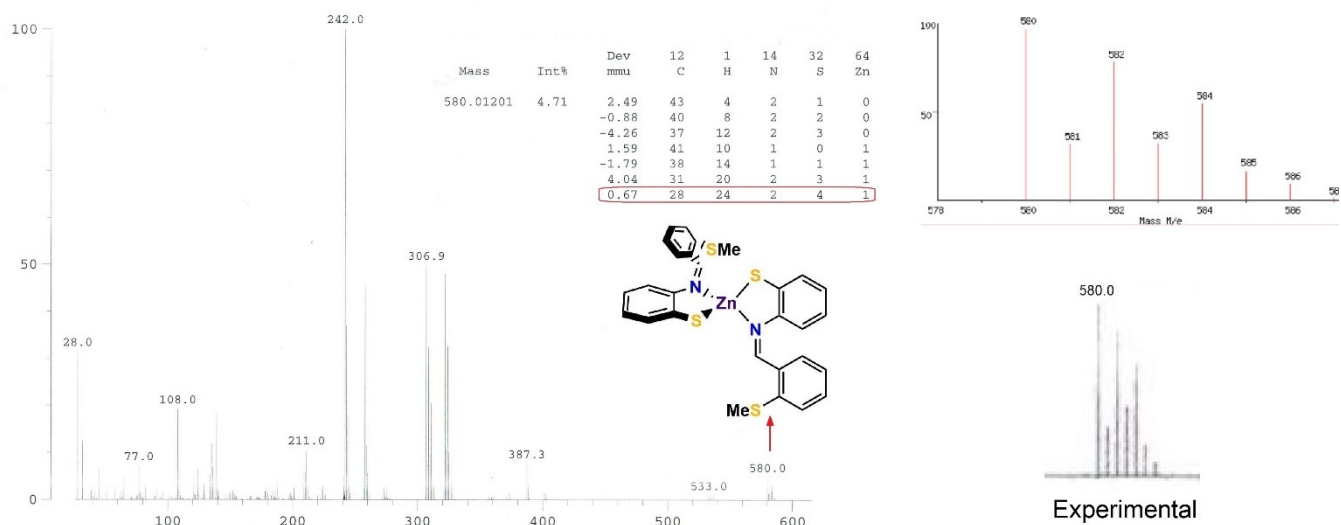


**Figure S29.** EI-MS spectrum of  $Zn(L^2)_2$  showing  $[M^+]$ .

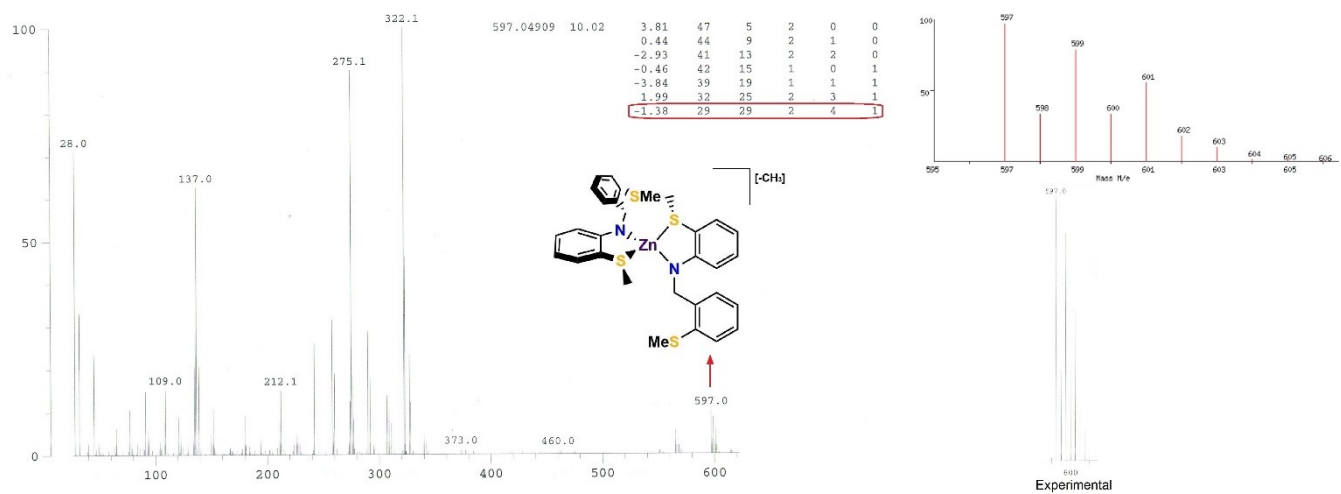


**Figure S30.** EI-MS spectrum of  $Zn(L^1)_2$  showing  $[M-CH_3]^+$ .

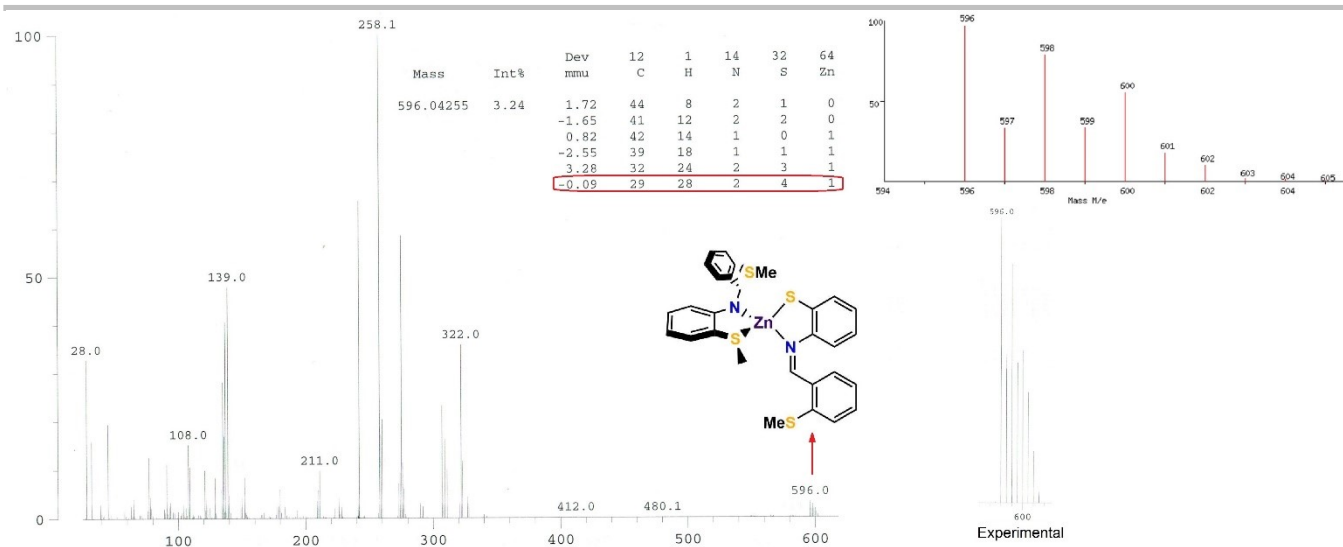


**Figure S31.** EI-MS spectrum of Zn(L<sup>1</sup>)(L<sup>2</sup>) showing [M<sup>+</sup>].

## 8. X-ray Diffraction Data

Crystallographic data were collected from single crystals mounted on MiTeGen dual thickness MicroMounts using Parabar oil. Data were collected on a Bruker Smart ApexII single crystal diffractometer equipped with a graphite monochromator. The instrument was equipped with a sealed tube Mo  $K\alpha$  source ( $\lambda = 0.71073 \text{ \AA}$ ), an ApexII CCD detector and a dry compressed air cooling system. All samples were cooled to 203(2) K during data collection. Raw data collection and processing were performed with the Apex3 software package from Bruker.<sup>[5]</sup> Initial unit cell parameters were determined from 36 data frames from select  $\omega$  scans. Semi-empirical absorption corrections based on equivalent reflections were applied.<sup>[6]</sup> Systematic absences in the diffraction data-set and unit-cell parameters were consistent with the assigned space group. The initial structural solutions were determined using ShelxT direct methods<sup>[7]</sup>, and refined with full-matrix least-squares procedures based on  $F^2$  using ShelXL or ShelXle.<sup>[8]</sup> Compound N-borylated L<sup>1</sup> exhibited minor positional disorder which was refined in ShelXle. Hydrogen atoms were placed geometrically and refined using a riding model.

**Table S1.** X-ray crystallographic data collection and refinement details.

	Zn(L <sup>1</sup> ) <sub>2</sub> (S0707)	Zn(L <sup>2</sup> ) <sub>2</sub> (S0699)	Zn(L <sup>1</sup> )(L <sup>2</sup> ) (S0811)	N-Borylated L <sup>1</sup> (S0733)	P <sup>1</sup> (S0927)
<b>empirical formula</b>	C <sub>30</sub> H <sub>32</sub> N <sub>2</sub> S <sub>4</sub> Zn	C <sub>28</sub> H <sub>24</sub> N <sub>2</sub> S <sub>4</sub> Zn	C <sub>29</sub> H <sub>28</sub> N <sub>4</sub> S <sub>4</sub> Zn	C <sub>21</sub> H <sub>28</sub> BNO <sub>2</sub> S <sub>2</sub>	C <sub>21</sub> H <sub>19</sub> NS <sub>2</sub>
<b>formula weight (g<math>\hat{\text{a}}</math>...mol<sup>-1</sup>)</b>	614.18	582.10	598.14	401.37	349.49
<b>crystal system</b>	orthorhombic	monoclinic	triclinic	Monoclinic	orthorhombic
<b>space group</b>	<i>Pbcn</i>	<i>P2<sub>1</sub>/c</i>	<i>P1</i>	<i>P2<sub>1</sub>/c</i>	<i>Pna2<sub>1</sub></i>
<b>a (A)</b>	21.2905(10)	7.1899(7)	10.7382(9)	10.9771(4)	18.558(3)
<b>b (A)</b>	7.6279(4)	8.1002(8)	11.2465(11)	11.5337(4)	9.2607(14)
<b>c (A)</b>	17.5124(8)	44.714(4)	12.8901(12)	17.6262(6)	10.3515(16)
<b><math>\hat{\text{I}}_{\pm}</math> (deg)</b>	90	90	68.170(3)	90	90
<b><math>\hat{\text{I}}_{-}</math> (deg)</b>	90	94.341(3)	68.707(3)	104.460(1)	90
<b><math>\hat{\text{I}}_{-}</math> (deg)</b>	90	90	87.560(3)	90	90
<b>V (A<sup>3</sup>)</b>	2844.0(2)(7)	2596.7(4)	1338.7(2)	2160.90(13)	1779.0(5)
<b>Z</b>	4	4	2	4	4
<b>T (K)</b>	203(2)	203(2)	203(2)	203(2)	203(2)
<b><math>\hat{\text{I}}_{\text{calcd}}</math> (g<math>\hat{\text{a}}</math>...cm<sup>-3</sup>)</b>	1.434	1.489	1.484	1.234	1.305
<b><math>\hat{\text{I}}_{-}</math> (mm<sup>-1</sup>)</b>	1.180	1.288	1.252	0.262	0.301
<b><math>2\hat{\text{I}}_{\text{max}}</math> (deg)</b>	61.012	55.298	55.444	52.844	51.408
<b>total/unique reflections</b>	25606/4339	63086/6027	28566/6216	16576/4421	10688/3304
<b>Reflections [<math>\hat{\text{I}}_{\text{o}}</math> <math>\hat{\text{a}}</math>%<math>\hat{\text{I}}_{\text{o}}</math> <math>\hat{\text{I}}_{\text{o}}</math> <math>\hat{\text{I}}_{\text{o}}</math>]</b>	2853	3745	4286	3121	2681
<b><math>R_1, wR_2</math> [<math>\hat{\text{I}}_{\text{o}}</math> <math>\hat{\text{a}}</math>%<math>\hat{\text{I}}_{\text{o}}</math> <math>\hat{\text{I}}_{\text{o}}</math> <math>\hat{\text{I}}_{\text{o}}</math>]</b>	0.0408, 0.0821	0.0441, 0.685	0.0419, 0.0748	0.0502, 0.1280	0.0588, 0.1415
<b>goodness of fit</b>	1.022	1.005	1.005	1.055	1.034

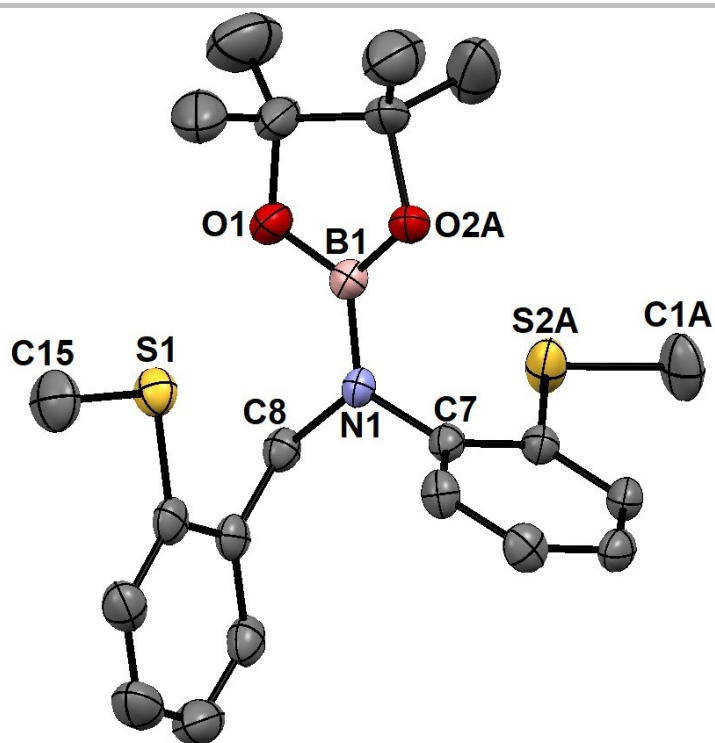


**Figure S32.** Molecular structure of *N*-borylated L<sup>1</sup> with 50% probability thermal ellipsoids and hydrogen atoms omitted for clarity.

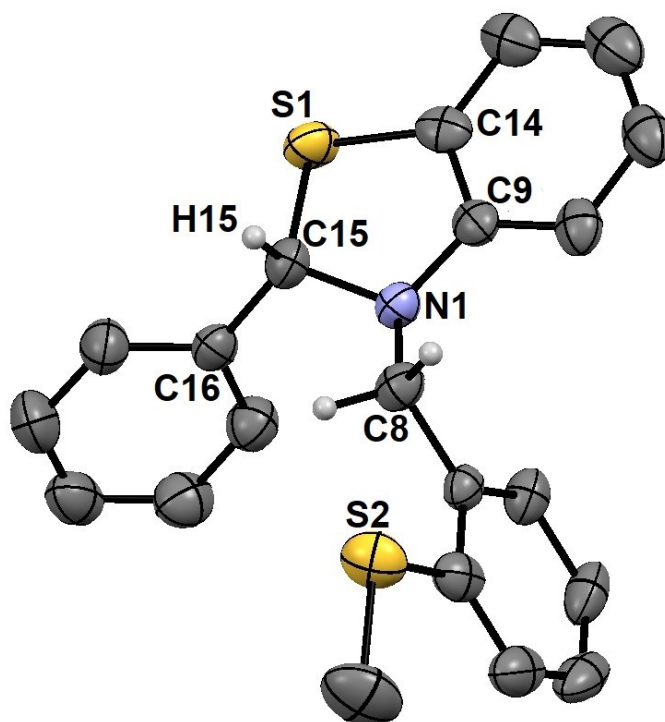


**Figure S33.** Molecular structure of P<sup>1</sup> with 50% probability thermal ellipsoids and hydrogen atoms omitted for clarity.

---

**Table S2.** Bond lengths for Zn(L<sup>1</sup>)<sub>2</sub>.

<b>Atom</b>	<b>Atom</b>	<b>Length/Å</b>
Zn1	S1	2.4663
Zn1	N1	1.925
Zn1	S1	2.4663
Zn1	N1	1.925
S1	C1	1.818(2)
S1	C2	1.780(2)
S2	C14	1.771(2)
S2	C15	1.789(3)
N1	C7	1.361(3)
N1	C8	1.453(3)
C2	C3	1.386(3)
C2	C7	1.422(3)
C3	C4	1.377(4)
C4	C5	1.382(4)
C5	C6	1.375(3)
C6	C7	1.423(3)
C8	C9	1.511(3)
C9	C10	1.393(3)
C9	C14	1.398(3)
C10	C11	1.376(4)
C11	C12	1.372(4)
C12	C13	1.388(4)
C13	C14	1.390(3)
S1	C1	1.818(2)
S1	C2	1.780(2)
S2	C14	1.771(2)
S2	C15	1.789(3)
N1	C7	1.361(3)
N1	C8	1.453(3)
C2	C3	1.386(3)
C2	C7	1.422(3)
C3	C4	1.377(4)
C4	C5	1.382(4)
C5	C6	1.375(3)
C6	C7	1.423(3)
C8	C9	1.511(3)
C9	C10	1.393(3)
C9	C14	1.398(3)
C10	C11	1.376(4)
C11	C12	1.372(4)
C12	C13	1.388(4)
C13	C14	1.390(3)

---

**Table S3.** Bond lengths for Zn(L<sup>2</sup>)<sub>2</sub>.

<b>Atom</b>	<b>Atom</b>	<b>Length/Å</b>
Zn1	S1	2.273(1)
Zn1	S3	2.246(1)
Zn1	N1	2.085(2)
Zn1	N2	2.109(2)
S1	C14	1.755(3)
S2	C1	1.784(4)
S2	C2	1.755(3)
S3	C28	1.757(3)
S4	C15	1.798(3)
S4	C16	1.755(3)
N1	C8	1.281(4)
N1	C9	1.434(4)
N2	C22	1.284(4)
N2	C23	1.430(4)
C2	C3	1.386(5)
C2	C7	1.405(5)
C3	C4	1.369(6)
C4	C5	1.390(6)
C5	C6	1.390(5)
C6	C7	1.392(5)
C7	C8	1.462(4)
C9	C10	1.387(5)
C9	C14	1.405(4)
C10	C11	1.376(4)
C11	C12	1.385(4)
C12	C13	1.383(5)
C13	C14	1.398(4)
C16	C17	1.385(4)
C16	C21	1.417(4)
C17	C18	1.382(5)
C18	C19	1.385(5)
C19	C20	1.383(5)
C20	C21	1.381(5)
C21	C22	1.465(4)
C23	C24	1.391(4)
C23	C28	1.414(4)
C24	C25	1.382(5)
C25	C26	1.381(5)
C26	C27	1.375(5)
C27	C28	1.393(4)

---

**Table S4.** Bond lengths for Zn(L<sup>1</sup>)(L<sup>2</sup>).

<b>Atom</b>	<b>Atom</b>	<b>Length/Å</b>
Zn1	S1	2.4793(7)
Zn1	S3	2.256(1)
Zn1	N006	1.923(3)
Zn1	N007	2.106(2)
S1	C1	1.817(3)
S1	C2	1.780(4)
S2	C14	1.771(3)
S2	C15	1.789(4)
S3	C16	1.763(3)
S4	C28	1.765(4)
S4	C29	1.790(3)
N006	C7	1.364(3)
N006	C8	1.460(3)
N007	C21	1.430(5)
N007	C22	1.287(4)
C2	C3	1.386(4)
C2	C7	1.422(4)
C3	C4	1.379(6)
C4	C5	1.391(4)
C5	C6	1.376(4)
C6	C7	1.418(5)
C8	C9	1.504(3)
C9	C10	1.390(4)
C9	C14	1.406(5)
C10	C11	1.380(5)
C11	C12	1.374(5)
C12	C13	1.381(4)
C13	C14	1.396(4)
C16	C17	1.387(6)
C16	C21	1.404(5)
C17	C18	1.383(5)
C18	C19	1.385(5)
C19	C20	1.373(6)
C20	C21	1.395(5)
C22	C23	1.453(6)
C23	C24	1.397(5)
C23	C28	1.413(4)
C24	C25	1.385(6)
C25	C26	1.384(4)
C26	C27	1.373(5)
C27	C28	1.390(6)

---

**Table S5.** Bond lengths for N-Borylated L<sup>1</sup>.

<b>Atom</b>	<b>Atom</b>	<b>Length/Å</b>
S1	C14	1.763(2)
S1	C15	1.794(3)
O1	C16	1.459(4)
O1	B1	1.370(4)
N1	C7	1.436(3)
N1	C8	1.468(3)
N1	B1	1.408(4)
C2	C3	1.394(4)
C2	C7	1.398(3)
C2	S2A	1.78(1)
C3	C4	1.378(3)
C4	C5	1.375(3)
C5	C6	1.384(4)
C6	C7	1.385(3)
C8	C9	1.502(3)
C9	C10	1.414(4)
C9	C14	1.403(3)
C10	C11	1.364(4)
C11	C12	1.370(5)
C12	C13	1.383(5)
C13	C14	1.404(4)
C16	C17	1.557(5)
C16	C18	1.473(6)
C16	C19A	1.596(8)
B1	O2A	1.424(8)
O2A	C19A	1.46(1)
C1A	S2A	1.79(2)
C19A	C20A	1.54(2)
C19A	C21A	1.51(1)

---

**Table S6.** Bond lengths for P<sup>1</sup>.

<b>Atom</b>	<b>Atom</b>	<b>Length/Å</b>
S1	C14	1.764(6)
S1	C15	1.838(6)
S2	C1	1.789(8)
S2	C2	1.773(6)
N1	C8	1.451(7)
N1	C9	1.393(7)
N1	C15	1.480(7)
C2	C3	1.383(9)
C2	C7	1.407(8)
C3	C4	1.40(1)
C4	C5	1.350(9)
C5	C6	1.418(8)
C6	C7	1.374(8)
C7	C8	1.502(8)
C9	C10	1.391(8)
C9	C14	1.395(8)
C10	C11	1.398(8)
C11	C12	1.347(9)
C12	C13	1.40(1)
C13	C14	1.379(8)
C15	C16	1.497(8)
C16	C17	1.375(8)
C16	C21	1.387(8)
C17	C18	1.375(8)
C18	C19	1.371(9)
C19	C20	1.37(1)
C20	C21	1.381(9)

---

## 9. References

- [1] U. K. Das, S. L. Daifuku, S. I. Gorelsky, I. Korobkov, M. L. Neidig, J. J. Le Roy, M. Murugesu, R. T. Baker, *Inorg. Chem.* **2016**, 55, 987–997.
- [2] U. K. Das, S. L. Daifuku, T. E. Iannuzzi, S. I. Gorelsky, I. Korobkov, B. Gabidullin, M. L. Neidig, R. T. Baker, *Inorg. Chem.* **2017**, 56, 13766–13776.
- [3] D. J. Darensbourg, M. W. Holtcamp, G. E. Struck, M. S. Zimmer, S. A. Niezgodá, P. Rainey, J. B. Robertson, J. D. Draper, J. H. Reibenspies, *J. Am. Chem. Soc.* **1999**, 121, 107-116.
- [4] M. Arrowsmith, T. J. Hadlington, M. S. Hill, G. Kociok-Kohn, *Chem. Commun.* **2012**, 48, 4567-4569.
- [5] APEX Software Suite v 2010 Bruker AXS Inc. Madison Wisconsin USA, **2010**.
- [6] R. H. Blessing in An Empirical Correction for Absorption Anisotropy, *Acta Crystallogr.* **1995**, A51, 33–38.
- [7] G. M. Sheldrick in A Short History of SHELX, *Acta Crystallogr.* **2008**, A64, 112–122.
- [8] C. B. Hübschle, G. M. Sheldrick, B. Dittrich in *ShelXle*: a Qt graphical user interface for SHELXL. *J. Appl. Crystallogr.* **2011**, 44, 1281–1284.